

UNCLASSIFIED

AD 409 489

DEFENSE DOCUMENTATION CENTER

FOR

SCIENTIFIC AND TECHNICAL INFORMATION

CAMERON STATION, ALEXANDRIA, VIRGINIA



UNCLASSIFIED

NOTICE: When government or other drawings, specifications or other data are used for any purpose other than in connection with a definitely related government procurement operation, the U. S. Government thereby incurs no responsibility, nor any obligation whatsoever; and the fact that the Government may have formulated, furnished, or in any way supplied the said drawings, specifications, or other data is not to be regarded by implication or otherwise as in any manner licensing the holder or any other person or corporation, or conveying any rights or permission to manufacture, use or sell any patented invention that may in any way be related thereto.



ORA-63-9

63

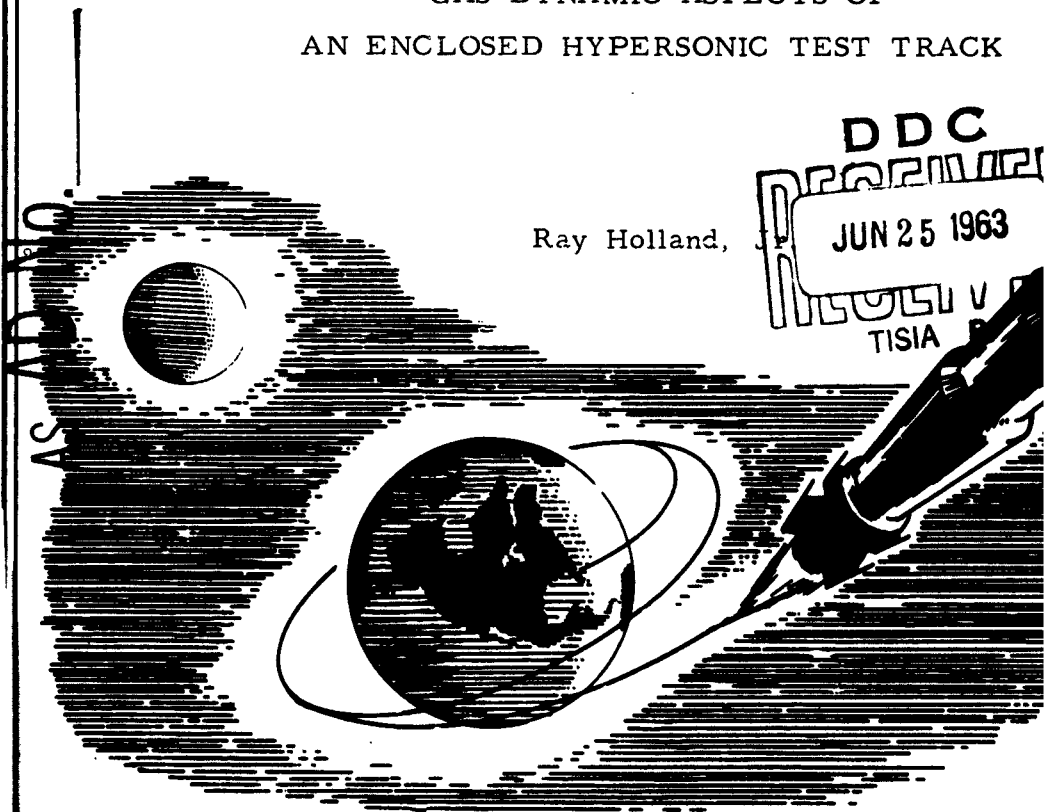
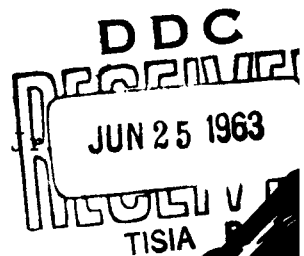
409 489

CATALOGED BY DDC 409489

HEADQUARTERS OFFICE OF AEROSPACE RESEARCH TECHNICAL REPORT

GAS DYNAMIC ASPECTS OF
AN ENCLOSED HYPERSONIC TEST TRACK

Ray Holland,



OFFICE OF RESEARCH ANALYSIS
HOLLOMAN AIR FORCE BASE
NEW MEXICO

May 1963

ORA-63-9

ORA-63-9

Project 5928

**GAS DYNAMIC ASPECTS OF
AN ENCLOSED HYPERSONIC TEST TRACK**

by

**Ray Holland, Jr.
Aeronautical Engineer
Research Associate
New Mexico Military Institute**

Consultant

Office of Research Analyses

**OFFICE OF AEROSPACE RESEARCH
UNITED STATES AIR FORCE
Holloman Air Force Base, New Mexico**

May 1963

FOREWORD

The author of this report, Mr. Raymond P. Holland, Jr., is a Research Associate at the New Mexico Military Institute at Roswell, New Mexico, and Consultant to the Office of Research Analyses at Holloman Air Force Base, New Mexico.

The report was prepared for the Track Test Division, Deputy for Guidance Test, Air Force Missile Development Center, Holloman Air Force Base, New Mexico, and supports Project 5928, Hypersonic Track Development. It provides information on the gas dynamics of a hypersonic track enclosed in an evacuated tube.

ABSTRACT

The gas dynamics related to the movement of a track-guided test vehicle through an evacuated tube are considered preliminarily. Values of pressure, temperature, density, and drag are computed for perfect piston action and for partial piston action at speeds up to the hypersonic. The effects of gas imperfections, viscosity, and wave-reflection are explored. The limiting conditions at which a body in a tube ceases to behave like a piston are defined.

At the lower limit of piston action, pressures, temperatures, and densities ahead of the vehicle are the same as for a flat-faced body in free air, and skin friction effects along the tube wall are negligible. At the upper limit of piston action, pressures in frictionless air range from about 44 percent greater (above Mach 8.0) to more than 80 percent greater (below Mach 2.0) than at the lower limit of piston action, and drag and heating due to friction predominate over shock effects; frictional heating in particular becomes large. The relative effects of piston action as compared to flow in free air are greater at low Mach numbers than at high Mach numbers. Pressures are ample at all speeds for effective braking by piston action, but high temperatures exist at all but the lowest speeds.

This report is approved for publication.


JAMES H. RITTER
Colonel, USAF

Commander, Office of Research Analyses

KEYWORDS

Tracks (Aerodynamics)

Ranges (Establishments)

Hypersonic Flow

Shock Waves

Supersonic Test Vehicles

Aerodynamic Heating

TABLE OF CONTENTS

	Page
SYMBOL LIST	xi
I. INTRODUCTION	1
II. METHOD	1
III. ANALYSIS	2
1. Perfect Piston Action. Perfect Gas. $\gamma = 1.4$	2
a. No Heat Loss	2
b. Arbitrary Heat Loss	5
c. Drag Coefficients	6
d. Reflected Shock Wave	10
2. Perfect Piston Action. Air with Viscosity	16
a. Drag Due to Skin Friction of Shock Layer	16
b. Temperature Rise Due to Skin Friction, Real Air	20
3. Imperfect Piston Action. Flow Past Piston or Through Orifices in Tube	23
a. Perfect Gas. $\gamma = 1.4$. No Heat Loss	23
b. Air with Viscosity	26
IV. RESULTS	28
1. Analytical Results	28
a. Perfect Piston Action. Perfect Gas. $\gamma = 1.4$	28
b. Perfect Piston Action. Air with Viscosity	29
c. Imperfect Piston Action	29
2. Physical Description	30
3. Discussion of Practical Aspects	47
V. CONCLUSIONS	52
REFERENCES	75

LIST OF ILLUSTRATIONS

Table	Page
I. Perfect Piston Action	54
II. Imperfect Piston Action	55
Figure	
1a. Velocity of normal shock wave relative to the air entering the shock. Variation with piston velocity. Perfect gas. $M_p = 0$ to $M_p = 20$	56
1b. $M_p = 0$ to $M_p = 4.0$	57
1c. $M_p = 0$ to $M_p = 1.0$	58
2. Velocity of normal shock wave relative to driving surface. (Driving surface is piston face when shock is forward-running, and is closed end of tube when shock is rearward-running.) Variation with piston velocity. Perfect gas. $\gamma = 1.4$	59
3a. Variation of absolute pressure ratio on front face of piston with piston velocity. Perfect gas. $\gamma = 1.4$ $M_p = 0$ to $M_p = 20$	60
3b. $M_p = 0$ to $M_p = 4.0$	61
3c. $M_p = 0$ to $M_p = 1.0$	62
4a. Variation of absolute temperature ratio in the shock layer ahead of the piston with piston velocity. Perfect gas. $\gamma = 1.4$ $M_p = 0$ to $M_p = 20$	63
4b. $M_p = 0$ to $M_p = 4.0$	64
5. Variation of the density ratio in the shock layer with piston velocity. Perfect gas. $\gamma = 1.4$	65
6. Variation of drag coefficient with piston velocity, assuming ambient pressure on rear face of piston. $M_p < 1.0$. Perfect gas. $\gamma = 1.4$. Long tube	66

Figure		Page
7.	Variation of drag coefficient with piston velocity, based on front face pressure only. $M_p > 1.0$. Perfect gas. $\gamma = 1.4$	67
8.	Variation of drag coefficient with shock wave velocity. Comparison with values obtained by computing rate of change of momentum, plastic pickup of mass	68
9.	Effect of reflected waves on drag coefficients for piston velocities from $M_p = .25$ to $M_p = 4.0$. Perfect gas. $\gamma = 1.4$. No heat loss. Perfect piston	69
10.	Approximate variation of the initial time rate of change of frictional drag coefficient with piston velocity, in ten-foot diameter tube at standard sea level ambient temperature. Perfect piston	70
11.	Approximate variation with piston velocity of the initial time rate of change of the mean frictional temperature rise in the shock layer. Perfect piston.	71
12.	Velocity of normal shock wave relative to driving surface for various degrees of piston imperfection. Variation with piston velocity. Perfect gas. $\gamma = 1.4$	72
13.	Maximum allowable orifice area ratio for normal shock piston action. (Lower limit of regime of piston action in a tube.) Variation with piston velocity. Perfect gas. $\gamma = 1.4$	73

SYMBOLS

A = area, ft^2

A_G = area, effective sum of frontal gap around piston and orifices or venting in tube in contact with shock layer, ft^2

A_P = area, frontal, piston or body in tube, ft^2

A_T = area, tube cross section, ft^2

a = velocity of sound, ft/sec

a_1 = velocity of sound in air at rest in the tube upstream from the shock wave, ft/sec

a_2 = velocity of sound in shock layer, ft/sec

C_D = drag coefficient, based on piston velocity, piston frontal area, and the density of the undisturbed air

C_{D_I} , $\frac{p_2 - p_1}{q}$ = pressure coefficient of the piston at subsonic speeds

$C_{D_{II}}$, $\frac{p_2}{q}$ = pressure coefficient of the piston at supersonic speeds

C_{D_f} = skin friction drag coefficient based on piston velocity, the area of the tube between the piston and the shock wave in rubbing contact with the shock layer, and the air density behind the shock wave.

C_{D_F} = skin friction drag coefficient based on piston velocity, piston frontal area, and the density of undisturbed air

C_p = specific heat of air at constant pressure

$C_p = 6006 \text{ ft}^2/\text{sec}^2/^{\circ}\text{R}$ (or $\text{ft}/\text{lb}/\text{slug}/^{\circ}\text{R}$) unless otherwise specified.

C_v = specific heat of air at constant volume

D = drag, pounds

D_f = drag, skin friction, pounds

d = diameter of tube, feet

$K_T = \frac{a_1^2}{2C_p T_1}$ = constant for determining stagnation temperature T

$$T_t = T_1(1 + K_T M_p^2)$$

L = length of tube, feet

M = Mach number

$M_p, V_p / a_1$ = Mach number of piston based on undisturbed air upstream from shock wave

$M_R, M_p + M_Q, V_R / a_1$ = Mach number, returning shock wave, reflected from the closed end of the tube, relative to the air entering the shock

$M_S, V_S / a_1$ = Mach number of forward running shock wave relative to piston

$M_Q, V_Q / a_1$ = Mach number of reflected shock wave, relative to the closed end of the tube

$M_W, M_p + M_S, V_W / a_1$ = Mach number of forward running shock wave relative to undisturbed air upstream

m = mass

n = completed cycles of shock-wave reflection

p = pressure, static, absolute, lb/ft²

$q = \frac{1}{2} \rho_1 V_p^2$ = dynamic pressure

R = gas constant, 1716 ft²/sec² per degree Rankine

S = area, rubbing contact, ft²

S_2 = area, rubbing contact, shock layer on tube wall, ft²

T = temperature, absolute, Rankine or Fahrenheit

$^{\circ}\text{Rankine} = ^{\circ}\text{Fahrenheit} + 459.6^{\circ}$

\bar{T} = temperature, absolute, thoroughly mixed air,

$^{\circ}\text{Rankine}$ or $^{\circ}\text{Fahrenheit}^{\circ}$

t = time, measured from $t = 0$ at instant piston enters tube

V = velocity, ft/sec

V_p = velocity, piston and shock layer ahead of piston, relative to tube, ft/sec

V_R = velocity, returning shock wave, reflected from closed end of tube, relative to air entering shock wave, ft/sec

V_S = velocity, shock wave relative to piston

V_Q = velocity, returning shock wave, reflected from closed end of tube, relative to closed end of tube

$V_W, V_p + V_S$ = velocity of shock wave relative to air at rest in tube upstream from shock wave

γ = ratio of specific heats at constant pressure and constant volume, constant at 1.4 unless otherwise specified

ρ = density, slugs/ft³

*Temperatures are static temperatures as measured by a thermometer at rest relative to the air being measured.

Subscripts

- 1 = original conditions in tube in undisturbed air at rest relative to tube
- 2 = conditions in the shock layer, upstream from piston and downstream from shock
- 3 = conditions between a reflecting shock wave and the closed end of a tube from which it has reflected
- 4 = conditions at face of piston immediately following first reflection of shock wave from face
- F = frictional, based on piston frontal area
- f = frictional, based on rubbing surface area
- G = gap or orifice
- P = piston
- R = reflection
- S = shock wave, relative to piston
- T = tube
- t = total, conditions which would exist if air were brought to rest isentropically
- W = shock wave, relative to air at rest upstream

GAS DYNAMIC ASPECTS OF AN ENCLOSED HYPERSONIC TEST TRACK

I. INTRODUCTION

To obtain insight into the gas dynamics of an enclosed, evacuated, hypersonic test track, including the maximum temperatures, densities, and drag coefficients which may occur, a study was made of a body moving through a long tube over a range of constant velocities from zero to Mach 20. The effect of air escape past the body or outward through orifices in the tube wall was considered. Attention was directed to the possible use of a tube for braking.

II. METHOD

Methods of analysis were selected primarily to gain perspective. Shock phenomena for a perfect piston were analyzed using the relationships for a normal shock wave in a perfect gas, first without heat loss from the system and then, to simulate imperfect gas or heat loss effects, the temperature in the shock layer was made equal to free stream stagnation temperature. Drag coefficients were computed from the pressures obtained at the front face of the piston. Reflected shocks from a closed tube-end were considered on the same basis. Viscous effects were considered by superimposing skin friction on the perfect gas results, using simplifying approximations with regard to Reynolds number, Mach number, and the distribution of the heat due to friction in the shock layer. Varying degrees of piston imperfection were considered for a perfect gas without heat loss by taking into account a loss of mass from the shock

layer by choked orifice flow. To permit the results to apply both to atmospheric and evacuated tubes, ratios were obtained; these ratios relate the conditions at the face of the piston to the conditions in the undisturbed air upstream.

In all cases the body moves at constant velocity without mechanical friction in a tube of constant diameter. The undisturbed air in the tube upstream from the shock wave is at constant temperature, pressure, and density; serial effects obtained by running through frangible diaphragms into air at different densities were not considered. The effect of the tube on the velocity of shock wave propagation was ignored.

III. ANALYSIS

1. Perfect Piston Action. Perfect Gas. $\gamma = 1.4$

a. No Heat Loss

The following relationships govern:

$$\frac{p_2}{p_1} = \frac{\rho_2}{\rho_1} \cdot \frac{T_2}{T_1} \quad \text{(equation of state)} \quad (1)$$

$$\frac{p_2}{p_1} = \frac{7M_W^2 - 1}{6} \quad \text{(static pressure ratio through a normal shock wave)} \quad (2)$$

$$\frac{T_2}{T_1} = \frac{(7M_W^2 - 1)(M_W^2 + 5)}{36 M_W^2} \quad \text{(static temperature ratio through a normal shock wave)} \quad (3)$$

$$\frac{\rho_2}{\rho_1} = \frac{V_W}{V_S} = \frac{M_W}{M_S} = \frac{M_W}{M_W - M_P} \quad (\text{conservation of mass}) \quad (4)$$

or

$$M_P = M_W \left(1 - \frac{\rho_1}{\rho_2} \right) \quad (\text{conservation of mass}) \quad (5)$$

and

$$M_W = M_P + M_S \quad (\text{by definition}) \quad (6)$$

See reference [1] for a convenient summary of the development of expressions (1) through (3) with particular reference to expressions (2), (93) and (95) therein. Expression (4) is obtained by considering the mass flow rate through sections across the tube moving with the shock wave, one just upstream and the other just downstream from the shock. This relationship in the form shown in expression (5) is discussed in reference [2], page 494.

From (1), (2), (3), and (4),

$$\frac{7M_W^2 - 1}{6} = \frac{\rho_2}{\rho_1} \cdot \frac{T_2}{T_1} = \frac{M_W}{M_W - M_P} \cdot \frac{(7M_W^2 - 1)(M_W^2 + 5)}{36 M_W^2}$$

from which

$$M_P = \frac{5(M_W^2 - 1)}{6 M_W} \quad (\text{no heat loss}) \quad (7)$$

or

$$M_W = \frac{6M_P + \sqrt{36M_P^2 + 100}}{10} \quad (\text{no heat loss}) \quad (8)$$

This relationship between piston speed and shock wave speed enables the quantities in expressions (2) through (6) to be obtained when the piston speed and the undisturbed conditions in the tube are known. For example, from (4)

$$\frac{\rho_1}{\rho_2} = \frac{M_W - M_P}{M_W} = 1 - \frac{M_P}{M_W}$$

and from (7)

$$\frac{M_P}{M_W} = \frac{5(M_W^2 - 1)}{6M_W^2}$$

so that

$$\frac{\rho_1}{\rho_2} = \frac{M_W^2 + 5}{6M_W^2} \quad (9)$$

or

$$\frac{\rho_1}{\rho_2} = \frac{6M_W^2}{M_W^2 + 5} \quad (10)$$

It is evident from expression (9) that as the velocity of the shock wave increases the density jump through the shock approaches 6:1,

the limiting density ratio across a normal shock in a perfect gas having $\gamma = 1.4$. Results are shown in solid lines on Figures 1 through 5, pages 56 through 65, and in Table I, page 54.

- b. Arbitrary Heat Loss. T_2 = stagnation temperature. No friction.
Ambient temperature. S. L. standard

The heat loss is assumed to be sufficient to limit the temperature in the shock layer to that due only to the conversion to heat of the kinetic energy of the stream at piston velocity, without the additional temperature rise (included in (a) above) caused by the compression of the air as it crosses the shock front. The temperature is now the total or stagnation temperature, and the temperature rise is obtained by dividing the kinetic energy of one slug of air, $1/2 V_p^2$, by the specific heat of air at constant temperature, so that

$$T_t = T_1 + \frac{V_p^2}{2C_p} = T_1 + \frac{a_1^2 M_p^2}{2C_p} \quad (11)$$

or when $T_2 = T_t$,

$$\frac{T_2}{T_1} = 1 + K_T M_p^2 \quad (12)$$

where

$$K_T = \frac{a_1^2}{2T_1 C_p} = \frac{a_1^2}{12012 T_1}$$

Using standard sea level conditions, $T_1 = 518.6$ °R, $a = 1117$ ft/sec, and $K_T = .200$. From (1), (2), (4), and (12),

$$\frac{7M_W^2 - 1}{6} = \frac{\rho_2}{\rho_1} \frac{T_2}{T_1} = \frac{M_W(1 + .2 M_P^2)}{M_W - M_P} \quad (13)$$

or

$$M_P = \frac{1 - 7M_W^2 + \sqrt{82.6 M_W^4 - 47.6 M_W^2 + 1}}{2.4 M_W} \quad (14)$$

$T_2 = T_t \quad (T_2 = \text{stagnation temperature})$

enabling the quantities in expressions (2), (4), and (12) to be obtained when ambient conditions are known.

Results are shown in broken lines on Figures 1 through 5.

c. Drag Coefficients. Inviscid flow.

(1) By pressure relationships

For tubes which are open at the starting end, at piston velocities less than Mach 1.0,

$$C_{D_I} = \frac{P_2 - P_1}{q} \quad (15)$$

For tubes which are closed at the starting end and for open tubes at piston velocities greater than Mach 1.0,

$$C_{D_{II}} = \frac{P_2}{q} \quad (16)$$

When tubes are open at the starting end, full atmospheric pressure acts on the downstream face of the piston when the piston velocity is much less than the speed of sound, leading to expression (15). At piston velocities much greater than the speed of sound no atmospheric pressure can reach the downstream face of the piston, even with an open tube, leading to (16). At piston speeds near the speed of sound in the atmosphere, when the starting end of the tube is open, both expressions are approximations.

An expression for $C_{D_{II}}$, for the particular case when $\gamma = 1.4$, may be obtained from expressions (1) and (2) and the standard relationships $p_1 / \rho_1 = RT_1$, $a_1^2 = \gamma RT_1$, and $V_p = M_p a_1$:

$$C_{D_{II}} = 2 \left(\frac{7 M_W^2 - 1}{8.4 M_p^2} \right) \quad (17a)$$

For general values of γ , by considering the power $p_2 A V_p$ necessary to drive the piston, and applying the momentum theorem $p_2 = p_1 + \rho_1 V_W V_p$, the gas law, and the equations of continuity and energy, one obtains

$$\text{Power} = \rho_1 V_W A \left[\frac{V_p^2}{2} + C_V (T_2 - T_1) \right]$$

This expression can be rewritten using standard thermodynamic relationships to yield

$$\text{Power} = \rho_1 V_W A V_p^2 \cdot \frac{M_W^2 - \frac{\gamma - 1}{2\gamma}}{M_W^2 - 1}$$

from which

$$C_{D_{II}} = 2 \frac{M_W}{M_P} \cdot \frac{M_W^2 - \frac{\gamma - 1}{2\gamma}}{M_W^2 - 1} \quad (17b)*$$

Drag coefficients are plotted on Figures 6, 7, and 8, pages 66 through 68. Values for C_{D_I} are computed from expressions (2), (7) or (14), and (15), using $p_1 = 2116 \text{ lb/ft}^2$ and $\rho_1 = .00238 \text{ slugs/ft}^3$, corresponding to standard sea level conditions. When the tube is evacuated, lower values of both these quantities exist, but the results still apply because their ratio p_0/ρ_1 is constant at constant temperature, and the temperature in the tube is independent of its degree of evacuation.

(2) By plastic pickup of mass

Since the air in the shock layer is trapped within the tube between the piston and the shock wave, and moves at the constant velocity of the piston, the reaction on the front face of the piston may also be determined approximately by considering the rate at which mass is picked up and accelerated to constant velocity. This method is considered in detail below.

Mass at zero velocity is picked up in plastic collision by a body moving at velocity V_P and moves with that body at velocity V_P from point a to point b. If the mass of the body is m_0 and the

*The author is indebted to Dr. Harald Melkus for expression (17b).

mass gained is m_1 , the work done between points a and b is:

$$\begin{aligned} \text{Work} = & + \text{final kinetic energy of } m_0 + m_1 \\ & - \text{initial kinetic energy of } m_0 \\ & + \text{initial kinetic energy of } m_1 \text{ relative to } m_0 \end{aligned}$$

$$\text{Work} = \frac{1}{2} (m_0 + m_1) V_P^2 - \frac{1}{2} m_0 V_P^2 + \frac{1}{2} m_1 V_P^2 = m_1 V_P^2$$

and

$$\text{Power} = \frac{m_1}{t} V_P^2$$

where t is the time to move from a to b.

In a tube of cross-sectional area A , the mass of air of density ρ picked up per unit time t , through a shock wave moving with constant velocity V_W , is

$$\frac{m_1}{t} = \rho A V_W$$

so that

$$\text{Power} = \rho A V_W \cdot V_P^2 = \text{Drag} \cdot \text{Velocity} = D V_P$$

and the drag coefficient,

$$C_{D_{II}} = \frac{D}{qA} = \frac{\rho A V_P^2}{\frac{1}{2} \rho V_P^2 A} \cdot \frac{V_W}{V_P} = 2.0 \frac{V_W}{V_P}$$

or,

$$C_{D_{II}} = 2.0 \frac{M_W}{M_P} \quad (\text{by plastic pickup of mass}) \quad (18)$$

Comparison of expressions (18) and (17b) shows agreement at high Mach numbers.

Results are shown in dotted lines on Figure 8. The upper curves compare the results with the drag coefficients obtained in a perfect gas without heat loss and the lower curves compare the results obtained when the temperature in the shock layer ahead of the piston is the total or stagnation temperature.

d. Reflected Shock Wave. Closed tube. No friction.

(1) No heat loss

$$\frac{P_3}{P_2} = \frac{\rho_3 T_3}{\rho_2 T_2} \quad (\text{equation of state}) \quad (19)$$

$$\frac{P_3}{P_2} = \frac{7M_R^2 - 1}{6} \quad (\text{static pressure ratio across a normal shock wave}) \quad (20)$$

$$\frac{T_3}{T_2} = \frac{(7M_R^2 - 1)(M_R^2 + 5)}{36 M_R^2} \quad (\text{static temperature ratio across a normal shock wave}) \quad (21)$$

These expressions correspond directly to (1), (2), and (3) in Section III.1.a, above. In that analysis the shock and the piston

were moving in the same direction. Now, the shock has reflected from the closed end of the tube and is moving in a direction opposite to that of the piston. Therefore, the expression based on the continuity of mass flow, where V_Q is the velocity of the reflected wave relative to the closed end of the tube, is as follows:

$$\rho_3 V_Q = \rho_2 (V_Q + V_P)$$

or

$$\frac{\rho_3}{\rho_2} = \frac{V_Q + V_P}{V_Q} = \frac{M_Q + M_P}{M_Q} \quad (22)$$

And, the velocity M_R of the returning shock wave relative to the air moving in front of the piston

$$M_R = M_P + M_Q \quad (23)$$

so that

$$\frac{\rho_3}{\rho_2} = \frac{M_R}{M_R - M_P}$$

Therefore, from (19),

$$\frac{7M_R^2 - 1}{6} = \frac{M_R}{M_R - M_P} \cdot \frac{(7M_R^2 - 1)(M_R^2 + 5)}{36 M_R^2}$$

and

$$M_P = \frac{5(M_R^2 - 1)}{6M_R} \quad (24)$$

and

$$\frac{\rho_3}{\rho_2} = \frac{6M_R^2}{M_R^2 + 5} \quad (25)$$

From expressions (7) and (10) it will be seen that

$$M_R = M_W \quad (\text{but in the opposite direction}) \quad (26)$$

and from (6) and (23)

$$M_Q = M_S \quad (\text{but in the opposite direction}) \quad (27)$$

and

$$\frac{\rho_3}{\rho_2} = \frac{\rho_2}{\rho_1} \quad (28)$$

$$\frac{p_3}{p_2} = \frac{p_2}{p_1} \quad (29)$$

$$\frac{T_3}{T_2} = \frac{T_2}{T_1} \quad (30)$$

The values of M_R may be found from Figure 1 when M_P is known, after which expressions (2), (21), and (25) (or (2), (3), and

(4)) may be used to obtain the pressure, temperature, and density, p_3 , T_3 , and ρ_3 , respectively, between the reflecting shock wave and the closed end of the tube. The values of the corresponding quantities between the reflecting shock wave and the piston (p_2 , T_2 , and ρ_2) would have been previously obtained from Section III.1.a, above.

When the reflected shock wave reaches the piston, the values of p_3 , T_3 , and ρ_3 act at the piston only instantaneously and then increase again to p_4 , T_4 , and ρ_4 in a re-reflection. For analysis of the re-reflection the equations of Section III.1.a apply exactly as in the original non-reflected case, except that $\frac{p_4}{p_3}$, $\frac{T_4}{T_3}$, and $\frac{\rho_4}{\rho_3}$ replace $\frac{p_2}{p_1}$, $\frac{T_2}{T_1}$, and $\frac{\rho_2}{\rho_1}$, respectively.

As the shock wave continues to reflect back and forth, the steps indicated above repeat and the pressures, temperatures, and densities increase by jumps as the shock wave passes, leading to the following considerations:

Let z represent p , T , or ρ .

Then at the end of one full cycle of shock wave reflection (one reflection each from the end of the tube and from the piston)

$$\frac{z_4}{z_1} = \frac{z_2}{z_1} \cdot \frac{z_3}{z_2} \cdot \frac{z_4}{z_3}$$

and at the end of two full cycles,

$$\frac{z_6}{z_1} = \frac{z_2}{z_1} \cdot \frac{z_3}{z_2} \cdot \frac{z_4}{z_3} \cdot \frac{z_5}{z_4} \cdot \frac{z_6}{z_5}$$

and from (2), (3), and (20), (21) and (26), (27), (28), (29), and (30),

$$\frac{z_2}{z_1} = \frac{z_3}{z_2} = \frac{z_4}{z_3} = \frac{z_5}{z_4} \dots$$

so that

$$\frac{z_4}{z_1} = \left(\frac{z_2}{z_1} \right) \left(\frac{z_2}{z_1} \right)^2 = \left(\frac{z_2}{z_1} \right)^{2n+1}$$

and

$$\frac{z_6}{z_1} = \left(\frac{z_2}{z_1} \right) \left(\frac{z_2}{z_1} \right)^4 = \left(\frac{z_2}{z_1} \right)^{2n+1}$$

where n is the number of full cycles of shock reflection. In general the condition at the piston

$$z_P = z_1 \left(\frac{z_2}{z_1} \right)^{2n+1}$$

so that, from (2), (3), (10), and (16)

$$p_P = p_1 \left(\frac{7M_W^2 - 1}{6} \right)^{2n+1} \quad (31)$$

$$T_P = T_1 \left[\frac{(7M_W^2 - 1)(M_W^2 + 5)}{36 M_W^2} \right]^{2n+1} \quad (32)$$

and from (2), (3), and (20), (21) and (26), (27), (28), (29), and (30),

$$\frac{z_2}{z_1} = \frac{z_3}{z_2} = \frac{z_4}{z_3} = \frac{z_5}{z_4} \dots$$

so that

$$\frac{z_4}{z_1} = \left(\frac{z_2}{z_1} \right) \left(\frac{z_2}{z_1} \right)^2 = \left(\frac{z_2}{z_1} \right)^{2n+1}$$

and

$$\frac{z_6}{z_1} = \left(\frac{z_2}{z_1} \right) \left(\frac{z_2}{z_1} \right)^4 = \left(\frac{z_2}{z_1} \right)^{2n+1}$$

where n is the number of full cycles of shock reflection. In general the condition at the piston

$$z_P = z_1 \left(\frac{z_2}{z_1} \right)^{2n+1}$$

so that, from (2), (3), (10), and (16)

$$p_P = p_1 \left(\frac{7M_W^2 - 1}{6} \right)^{2n+1} \quad (31)$$

$$T_P = T_1 \left[\frac{(7M_W^2 - 1)(M_W^2 + 5)}{36 M_W^2} \right]^{2n+1} \quad (32)$$

$$\rho_P = \rho_1 \left(\frac{6M_W^2}{M_W^2 + 5} \right)^{2n+1} \quad (33)$$

$$C_{D_{II}} = \frac{P_P}{q} = \frac{P_1}{q} \left(\frac{7M_W^2 - 1}{6} \right)^{2n+1} \quad (34)$$

Values of expressions (31), (32), (33), and (34) increase by jumps at whole values of n , at the instant the reflected wave reaches the piston, and they remain constant until n increases by 1.0 at the next arrival of the reflected wave.

Expression (34) is plotted on Figure 9, page 69, for values of M_P from .125 to 4.0, up to four cycles of wave reflection.

(2) Arbitrary heat loss. T_2 = stagnation temperature.

It may be seen from the analysis III.1.d(1) above that expressions (31), (33), and (34) also apply in cases in which each rise of static temperature with the passage of a shock wave is limited to that which can be attributed solely to the conversion of kinetic energy to heat. This is equivalent to the assumption that the additional temperature rise due to additional compression of the air in the shock layer caused by mass accumulation in that layer is offset exactly by a loss of heat from the system. It is only necessary to use the proper values of M_W , those indicated on Figure 1 by T_2 = stagnation temperature, to apply these expressions. However, the expression for temperature is different.

From (12)

$$T_p = T_1 \left[1 + \frac{a_1^2 M_p^2}{12012 T_1} \right]^{2n+1} \quad (35)$$

2. Perfect Piston Action. Air With Viscosity.

a. Drag Due to Skin Friction of Shock Layer

The area, S_2 , of the rubbing surface at the boundary of the shock layer in contact with the walls of a circular tube grows at a steady rate from time $t = 0$ when the piston enters the tube, such that

$$S_2 = \pi d V_S t$$

The skin friction drag D_f between the shock layer and the walls of the tube is

$$\begin{aligned} D_f &= C_{D_f} \cdot \frac{1}{2} \rho_2 V_p^2 \cdot S_2 \\ &= C_{D_f} \cdot \frac{1}{2} \rho_2 V_p^2 \cdot \pi d V_S t \end{aligned} \quad (36)$$

Or,

$$D_f = C_{D_f} \frac{\rho_1}{2} V_p^3 \pi dt \cdot \frac{\rho_2}{\rho_1} \cdot \frac{M_S}{M_p} \quad (37)$$

Replacing C_{D_f} with a drag coefficient C_{D_F} based on the sectional area of the tube, A , an expression of familiar form is used

in which, however, C_{D_F} varies with time:

$$D_f = C_{D_F} \cdot \frac{\rho_1}{2} V_P^2 \cdot A$$

When the tube is circular, $A = \frac{\pi d^2}{4}$ and

$$D_f = C_{D_F} \cdot \frac{\rho_1}{2} V_P^2 \frac{\pi d^2}{4} \quad (38)$$

From (37) and (38)

$$C_{D_F} = \frac{4V_P}{d} \frac{\rho_2}{\rho_1} \frac{M_S}{M_P} C_{D_f} t$$

and since $V_P = a_1 M_P$ and (for perfect pistons) $\frac{\rho_2}{\rho_1} = \frac{M_W}{M_S}$ (from (4))

$$C_{D_F} = \frac{4a_1}{d} M_W C_{D_f} t = \frac{4V_W}{d} C_{D_f} t \quad (39)$$

$$\frac{dC_{D_F}}{dt} = \frac{4a_1}{d} M_W C_{D_f} \quad (40)$$

$t \approx 0$

$$D_F = \frac{4a_1}{d} M_W C_{D_f} q A_P t \quad (41)$$

$$\text{with } q = \frac{\rho_1}{2} V_P^2$$

Expressed in terms of piston speed, limited to the case of zero heat loss for perfect pistons from (8)

$$\frac{dC_{D_F}}{dt} = \frac{0.4 a_1}{d} \left(6M_P + \sqrt{36M_P^2 + 100} \right) C_{D_F} \quad (42)$$

$t \approx 0$

and

$$\frac{dD_F}{dt} = \frac{0.4 a_1}{d} \left(6M_P + \sqrt{36M_P^2 + 100} \right) C_{D_F} q A_P \quad (43)$$

$t \approx 0$

These relationships are limited to small values of time since the temperature in the shock layer will rise due to friction and will increasingly invalidate the basis of the analysis.

The skin friction drag coefficient, C_{D_F} , is a function of Reynolds number, Mach number, and the wall-to-free-stream temperature ratio. It varies with Reynolds number from about $C_{D_F} = .004$ for laminar flow at a Reynolds number of 10^5 to about $C_{D_F} = .0015$ for turbulent flow at a Reynolds number of 10^9 . It is not possible to include this variation in a simple analysis because the length dimension of the shock layer and hence its Reynolds number increases from zero at $t = 0$, linearly with time, reaching very high values; this occurs at any Mach number. Furthermore, the plug of air grows in a special manner, by rapidly accumulating air at its forward end, initially without a boundary layer, with the result that viscous effects such as boundary layer growth are not determined by body length in quite the usual way. The flow situation is a special case

of viscous effects in accelerated flow such as were studied preliminarily in reference [3]. For purposes of this analysis it is arbitrarily assumed that the Reynolds number is constant at a value of 10^8 .

The variation of C_{D_f} with Mach number, between $M = 0$ and $M = 16$, at $RN = 10^8$, may be approximated by

$$C_{D_f} = .002 - .0004M^{1/2} \quad (44)$$

This expression is based on reference [4], page 7-121, Figure 5, extrapolated from Mach 10.0 to Mach 16.0. A more accurate and more complex expression for C_{D_f} is not used in view of the inherent inaccuracies due to the Reynolds number, described above. The effect of wall temperature on C_{D_f} is also a function of Reynolds number and has been ignored.

Using (44), expressions (39) and (40) become (for perfect pistons)

$$C_{D_F} = \frac{4a_1}{d} M_W (.002 - .0004 M_P^{1/2}) t \quad (45)$$

$$\frac{dC_{D_F}}{dt} = \frac{4a_1}{d} (.002 - .0004 M_P^{1/2}) M_W \quad (46)$$

$t \approx 0$

Or, from (8) limited to the case of zero heat loss,

$$\frac{dC_{D_F}}{dt} = \frac{0.4 a_1}{d} \left(.002 - .0004 M_P^{1/2} \right) \left(6M_P + \sqrt{36M_P^2 + 100} \right) \quad (47)$$

$t \approx 0$

Assigning values to constants,

$a_1 = 1117 \text{ ft/sec}$, standard atmosphere at sea level,
corresponding to $T_1 = 59^\circ\text{F}$.

$d = 10 \text{ feet}$, a dimension selected on the high side of
expected values, to give drag results on
the low side.

From (46)

$$\frac{dC_{D_F}}{dt} = (.894 - .179 M_P^{1/2}) M_W \quad (48)$$

$t \approx 0$

Expression (48) is plotted on Figure 10, page 70, with the case of zero heat loss shown in solid line and the case of reduced temperature shown in dash line. The effect of the temperature rise due to friction may be inferred from the trend between these two curves. The trend of both curves toward reduced values at high Mach numbers is due to a decrease of skin friction drag coefficient, which is qualitatively correct but which is limited in accuracy by the assumptions previously described.

b. Temperature Rise Due to Skin Friction, Real Air

A temperature rise is caused in the shock layer by skin friction along the walls of the tube. This rise is locally intense adjacent to the walls, which remain relatively cool because of the high speed with which they stream past, causing a high rate of heat transfer into the wall material. This situation is complicated by the peculiar manner of growth

of the shock layer, by rapid accumulation at its forward end of air initially having no boundary layer. An accurate analysis of these actions would be complex and might obscure the principal point, which is to obtain some degree of insight into the magnitudes involved in the problem. For this purpose two simplifying assumptions of a counter-acting nature are used: (1) that no heat enters the walls, and (2) the heat which appears due to the work necessary to overcome skin friction is distributed uniformly throughout the mass of air in the shock layer. Then,

$$dW = D_f \cdot V_p \cdot dt$$

From (41)

$$\begin{aligned} \text{Work} &= \int_0^t \left(\frac{4a_1}{d} M_W C_{D_f} t \right) \left(\frac{1}{2} \rho_1 V_p^2 \right) \left(\frac{\pi d^2}{4} \right) \left(V_p \right) dt \\ &= \frac{a_1 M_W \pi d}{4} \rho_1 V_p^3 C_{D_f} t^2 \text{ ft/lb} \end{aligned}$$

The mass of air to which this energy is applied as heat is

$$\text{Mass} = \frac{\pi d^2}{4} \cdot \rho_2 V_S t \text{ slugs}$$

Using $C_p = 6006 \text{ ft/lb of work per slug of air per degree temperature rise, Rankine or Fahrenheit}$, the temperature rise of the air,

if well mixed, would be:

$$\begin{aligned}\bar{T} &= \frac{\text{Work}}{\text{Mass} \cdot C_p} \\ &= .0001665 \frac{a_1^3}{d} M_p^3 C_{D_f} t\end{aligned}$$

and

$$\left[\frac{d\bar{T}}{dt} \right]_{\substack{\text{friction} \\ t \approx 0}} = .0001665 \frac{a_1^3}{d} M_p^3 C_{D_f}$$

and from (44)

$$\left[\frac{d\bar{T}}{dt} \right]_{\substack{\text{friction} \\ t \approx 0}} = .0001665 \frac{a_1^3}{d} M_p^3 (.002 - .0004 M_p^{1/2})$$

And, for an example, when

$$a_1 = 1117 \text{ ft/sec}$$

$$d = 10 \text{ feet}$$

$$\frac{d\bar{T}}{dt} = 23205 (.002 - .0004 M_p^{1/2}) M_p^3 \quad (49)$$

Expression (49) is plotted in Figure 11, page 71.

3. Imperfect Piston Action. Flow Past Piston or Through Orifices in Tube

a. Perfect Gas. $\gamma = 1.4$. No Heat Loss.

The speed of sound,

$$a = \sqrt{\gamma RT}$$

And, from (3), the speed of sound in the shock layer, between the piston and a normal shock wave running in advance of the piston,

$$a_2 = \sqrt{\gamma RT_1} \sqrt{(7M_W^2 - 1)(M_W^2 + 5)} \cdot \frac{1}{6M_W} \quad (50)$$

The greatest velocity at which air will escape from the shock layer through a small gap between the piston and tube or through an orifice in the tube is the sonic speed in the escaping flow. Neglecting small changes in sonic speed and air density in acceleration to sonic velocity between the shock layer and the orifice, the maximum mass flow rate of escape from the shock layer is $\rho_2 A_G a_2$, where A_G is the total effective area of escape from the shock layer, including the effective gap around the piston and any effective vent area in the tube walls with which the shock layer is in contact. (The effective vent area may be less than the geometric vent area.)

The mass flow rate into the shock layer must equal the sum of the mass growth rate of the shock layer and the rate of mass escape from the shock layer. Assuming that air is escaping from the shock layer at

its maximum available rate,

$$P_1 A_T V_W = P_2 \left[A_T V_S + A_G a_2 \right] \quad (51)$$

where A_T is the cross-sectional area of the tube. Putting in non-dimensional form by dividing by a_1 , and using expression (6)

$$\frac{P_1}{P_2} = 1 - \frac{M_P}{M_W} + \frac{A_G}{A_T} \cdot \frac{a_2}{a_1} \cdot \frac{1}{M_W}$$

From (50)

$$\frac{P_1}{P_2} = 1 - \frac{M_P}{M_W} + \frac{A_G}{A_T} \cdot \frac{\sqrt{(7M_W^2 - 1)(M_W^2 + 5)}}{6M_W^2} \quad (52)$$

and from (1), (2), and (3),

$$\frac{6}{7M_W^2 - 1} = \frac{36M_W^2}{(7M_W^2 - 1)(M_W^2 + 5)} \left[1 - \frac{M_P}{M_W} + \frac{A_G}{A_T} \cdot \frac{\sqrt{(7M_W^2 - 1)(M_W^2 + 5)}}{6M_W^2} \right] \quad (53)$$

or

$$M_P = \frac{1}{6M_W} \left[5(M_W^2 - 1) + \frac{A_G}{A_T} \cdot \sqrt{(7M_W^2 - 1)(M_W^2 + 5)} \right] \quad (54)$$

The minimum piston speed for assuring normal shock action ahead of the piston occurs when $M_P = M_W$, at which time

$$\frac{A_G}{A_T} = \sqrt{\frac{M_P^2 + 5}{7M_P^2 - 1}} \quad \begin{array}{l} \text{(lower limit of piston action)} \\ M_P \geq 1.0 \end{array} \quad (55)$$

or

$$M_P = M_W = \left[\frac{\left(\frac{A_G}{A_T} \right)^2 + 5}{7 \left(\frac{A_G}{A_T} \right)^2 - 1} \right]^{1/2} \quad \begin{array}{l} \text{(lower limit} \\ \text{of piston action)} \\ M_P \geq 1.0 \end{array} \quad (56)$$

Values of M_W may be obtained from Table II, page 55, and from Figure 12, page 72, (since $M_W = M_G + M_P$) and from Figure 13, page 73, which are plotted from expressions (54) and (56), respectively, for use in expressions (2), (3), and (52) to obtain values of pressure, temperature, and density in cases of imperfect piston action. Values of drag due to frontal pressure, $p_2 A_P$, may also be computed.

At the lower limit of piston action (when $M_W = M_P$) the drag coefficient at standard sea level conditions, from (2)

$$C_{D_{II}} = \frac{p_2}{q} = \frac{2116(7M_P^2 - 1)}{6(.00119)(1117)^2 M_P^2}$$

$$C_{D_{II}} = 1.663 - \frac{.2375}{M_P^2} \quad (57)$$

b. Air with Viscosity

For frictional drag (from (37) and (38)):

$$C_{D_F} = \frac{\frac{4V_P}{d} \frac{M_S}{M_P} C_{D_f} t}{\rho_1 / \rho_2}$$

and from (52), since $V_P = a_1 M_P$

$$C_{D_F} = \frac{\left(\frac{4a_1}{d}\right) M_S C_{D_f} t}{1 - \frac{M_P}{M_W} + \frac{A_G}{A_T} \cdot \frac{\sqrt{\gamma R T_1}}{6M_W^2 a_1} \cdot \sqrt{(\gamma M_W^2 - 1)(M_W^2 + 5)}} \quad (58)$$

$t \approx 0$

(intermediate cases of imperfect piston action)

Entering Figure 12 with known values of A_G/A_T and M_P , the values of M_S and M_W are obtained (since $M_W = M_S + M_P$). All other quantities in (58) are known from the conditions of the problem, from which the frictional drag force for small values of t may be obtained, using $D_F = C_{D_F} q A_P$.

For temperature effects, following Section III.2.b, the work to overcome skin friction:

$$\text{Work} = \frac{1}{2} C_{D_F} q A_P V_P t \quad \text{ft/lb}$$

is applied as heat to the mass of the air in the shock layer,

$$\text{Mass} = \frac{\pi d^2}{4} \rho_2 V_S t \text{ slugs}$$

producing the average temperature rise in the shock layer

$$\bar{T} = \frac{\frac{1}{2} C_{D_F} q A_P V_P t}{\frac{\pi d^2}{4} \rho_2 V_S t \cdot C_p}$$

or,

$$\bar{T} = \frac{C_{D_F}}{\pi d^2} \cdot \frac{M_P^3}{M_S} \cdot \frac{a_1^2 A_P}{6006} \quad \begin{array}{l} \text{(intermediate cases of} \\ \text{imperfect piston action)} \end{array} \quad (59)$$

$t \approx 0$

By using values of C_{D_F} in (59) from (58) and by using Figure 12 to find M_S , the value of the average temperature rise due to friction in the shock layer may be determined.

It may be seen from (58) and (59) that the frictional drag force and the temperature rise due to friction become zero at the lower limit of piston action when $M_W = M_P$ and $M_S = 0$. This assumes that the tube is entered at time $t = 0$, which assures that the shock layer could not have grown from a previous history in the tube. In any case, the frictional drag and temperature rise become zero when the tube venting is such that the shock falls back to the piston.

IV. RESULTS

1. Analytical Results

a. Perfect Piston Action. Perfect gas. $\gamma = 1.4$.

(1) No heat loss

Expression (8) shows the relationship of shock wave velocity to body velocity, enabling pressures, temperatures, densities and shock wave velocities relative to the body, to be computed by expressions (2), (3), (4), and (6), respectively. These results are shown in Table I, and in solid lines in Figures 1, 3, 4, 5, and 2, respectively. Drag coefficients as defined in expressions (15) and (16) are shown on Figures 6 and 7, in solid lines.

(2) Arbitrary heat loss, T_2 = stagnation temperature

The relationship of shock wave velocity to body velocity is given in expression (14), through which pressures, temperatures, densities, and shock wave velocities relative to the body may be computed by expressions (2), (3), (4), and (6), respectively. These results are shown in dashed lines in Figures 1, 3, 4, 5, and 2, respectively. Drag coefficients as defined in expressions (15) and (16) are shown on Figures 6 and 7 in dashed lines.

(3) Plastic pickup of mass

Figure 8 shows that drag coefficients computed by assuming plastic pickup of mass agree well at high Mach numbers with those computed by normal shock wave analysis.

(4) Reflected shock wave, closed tube

Expressions (31), (32), (33), (34), and (35), together with expressions (7) and (14) which are plotted in Figure 1 define the conditions after shock wave reflection. Figure 9 illustrates these trends as they affect the drag coefficient defined in expression (16).

b. Perfect Piston Action. Air with Viscosity.

Expression (40) shows the time rate of increase of the body drag coefficient due to friction, and Figure 10 shows results for two assumed cases. Figure 11 shows the approximate initial time rate of rise of the average temperature in the shock layer due to viscosity, for an assumed case, based on expression (49).

c. Imperfect Piston Action

Expression (54) shows the relationship between shock wave velocity and body velocity (see Table II and Figure 12), from which pressures, temperatures, densities and shock wave velocities relative to the body may be computed using expressions (2), (3), (52), and (6), respectively. Expressions (55) and (56) and Figure 13 define the conditions at the lower limit of piston action. Shock wave velocities, pressures, densities, and drag coefficients at the lower limit of piston action are shown in dotted lines in Figures 1, 3, 5, and 7, respectively. Expressions (57) and (58) show the drag coefficients due to shock wave action and viscosity, respectively, and expression (59) shows the temperature rise due to friction, for intermediate cases of imperfect piston action.

2. Physical Description

There are three major flow regimes associated with the movement of a body through a gas-filled tube: (1) the piston regime, characterized by a normal shock wave running ahead of the body, (2) the shock interference regime in which the shock wave has dropped back on the body, has become oblique, and reflects from the tube wall onto the body, and (3) the "free" regime in which oblique shock waves reflect from the walls of the tube and pass entirely behind the body.

This report is not concerned with regime (3) because here the tube cannot make its presence felt on the body. The tube must be of large diameter if the flow is to fall in the regime, especially at low supersonic Mach numbers or with long bodies typical of track-guided test vehicles.

Regime (2) is of practical interest, particularly from the standpoint of reduction of drag, modulation of drag, and the avoidance of troublesome aerodynamic irregularities. Yet it is a relatively complex regime. The flow around a long body of arbitrary form in an arbitrary position in the tube can be enormously complex, and yet an axisymmetrical body of special shape on the tube centerline can achieve a simple symmetry of wave patterns which results in the cancellation of wave drag (see reference [5]). This regime has not been treated in this report.

Primary attention is directed to regime (1) in which, to some degree, the body moving through the tube behaves like a piston. The starting point is that of a perfect piston, moving through a perfectly smooth impervious tube filled with air which behaves like a perfect gas.

At the first forward movement of a piston in a long tube a pressure disturbance moves forward through the tube at the speed of sound (a Mach wave) marking the boundary between air disturbed by the piston and undisturbed air ahead. If the piston continues to move at a small constant velocity, the air ahead of it is pushed forward at piston speed. The moving air has the form of a plug which grows at its forward end at sonic velocity causing the mass of the air which moves with the piston to grow at a high rate.

Since the piston speed is small and the rate of increase of momentum is large (due to the large rate of increase of mass), the force which must be applied to the piston to maintain its speed will be large compared to the dynamic pressure which the piston would experience in open air. In other words, under these conditions the drag coefficient of the piston is large. It may be seen further that the plug of air ahead of the piston rubs against the walls of the tube and a drag reaction occurs from this source.

When the piston moves through the tube at a higher velocity, the pressure in front of the piston increases, the temperature of the air being driven forward starts to rise due to compression, and the velocity of propagation of the pressure disturbance into still air increases correspondingly, and the Mach wave becomes a weak shock wave. At still higher piston velocities the shock wave intensifies further and moves faster, becoming a strong shock wave.

The same situation may be seen from another viewpoint. If the piston were moving at a supersonic Mach number in the open air, it would

be preceded by a normal shock wave moving into undisturbed air at the same velocity as the piston. Air passing through this shock wave would find its way past the piston and would proceed downstream. Now, if the piston were encased in a tube which prevented air from passing the piston, the air which passed through the shock wave would accumulate between the shock wave and the piston, and consequently the shock wave would have to move upstream at a velocity higher than piston velocity.

The changes in velocity, pressure, density, and static temperature across a normal shock wave are independent of the source generating the shock wave: for instance they are the same for two shock waves moving at the same velocity into still air even though one of the shock waves is caused by a blunt body moving in open air at shock wave velocity and the other is caused by a growing plug of air. The latter is set in motion by a piston which moves at speeds smaller than the velocity of the shock wave.

To compute the conditions in the tube, therefore, the relationships for static pressure, static temperature and density across a normal shock wave may be used. These relationships are functions of shock wave velocity and not piston velocity. It is necessary, therefore, to determine the relationship between piston velocity and shock wave velocity.

The shock wave may be considered to be stationary with air flowing into the shock with a velocity equal to the shock wave velocity from the upstream side, and flowing out of the shock at the velocity at which the piston recedes downstream from the shock. The piston must withdraw from the shock to make space for air to accumulate between the piston and

the shock. The air density behind the shock is greater than in front, and the same mass of air flows into and out of the shock during the same time. From the density ratio across the shock (expression (4)) the piston velocity relative to the shock is obtained (expression (7)).

The original undisturbed air in the tube provides a convenient reference for making velocities non-dimensional. All velocities are expressed as Mach numbers, as ratios to the speed of sound in this undisturbed air, which is constant for any given set of initial conditions.

The air behind the normal shock wave has various properties. The flow there is always subsonic; no new shocks form in this region - the temperature and the local sonic speed of this region are sufficiently high to prevent their formation (except by reflection, as will be discussed later). Furthermore, when the air in the shock layer is considered to be frictionless and is pushed by a piston without leakage, all the air in the shock layer moves at piston velocity. There are no local flows, no streamlines, and no pressure gradients. Since zero heat loss is assumed, temperature and density are also uniform throughout this region.

In contrast to the familiar sensitive aerodynamic flow over bodies in the open air at transonic speeds, nothing irregular occurs at the front face of a piston moving a plug of perfect gas inside a tube at piston Mach numbers near 1.0. The Mach wave, which starts as an infinitely weak shock at very small piston velocity, increases in strength smoothly and progressively throughout the entire range of speeds and becomes a strong shock solely by changes of degree rather than by any change of physical phenomena.

This is a consequence of the fact that the shock does not occur at the piston face but at the front face of the advancing plug of air ahead of the piston, a face which is already moving at Mach 1.0 when the piston is barely moving.

The perfect gas analysis based on zero heat loss (Section III.1.a) shows that temperatures in the shock layer may be expected to become sufficiently high to render the assumption of a perfect gas invalid. Dissociation, ionization, and relaxation phenomena can be expected. No simple analysis can account for these effects (see references [6], [7], [8], and [9] for typical reports containing bibliographies in this area), but use may be made of the fact that imperfect gas effects cause energy relocations, absorbing energy from the kinetic model of the ideal gas, relatively increasing the specific internal energy and specific enthalpy, and reducing the temperature of the real gas. Therefore insofar as their relationship to a perfect gas analysis is concerned, imperfect gas effects may be represented qualitatively by a relative reduction of the temperature of the shock layer.

The practical reason for wishing to reduce shock layer temperature is to protect the test vehicle. The effect of a temperature reduction is therefore of interest in itself, particularly to learn how pressure values are affected. It was assumed that a practical amount for the reduced temperature in the shock layer is the total or stagnation temperature, such as would occur at the stagnation point on a body moving at piston velocity in free air. Using this value, the increment of temperature due to the presence of the tube could be assessed directly by comparing the solid line

and the broken line on Figure 4. This basis was therefore assumed for the analysis in Section III.1.b.

According to the basic analysis without heat loss (Section III.1.a), assuming ambient air at sea level standard temperature of 59°F, the temperature in the shock layer would be 5000°Rankine at a piston speed of Mach 5.5. The value of γ was assumed in this analysis to be constant at 1.4. At 5000°Rankine γ is not 1.4 but 1.29. If the latter value of γ is used to compute the pressure in the shock layer at Mach 5.5, a reduction of about 4 percent occurs. By assuming that the temperature in the shock layer is the stagnation temperature, as in the second analysis, a greater pressure reduction occurs at Mach 5.5, amounting to about 11 percent.

A qualitative comparison between the two analyses is available at higher Mach numbers by considering the density ratio across the shock. When the heat loss is zero and $\gamma = 1.4$, this ratio approaches 6.0 as a limit at high Mach numbers. With the assumed heat loss this value approaches 7.65; this is equivalent to a value of $\gamma = 1.3$ without heat loss for this particular item of comparison, a value which falls within the desired qualitative range.

Although computation of heat transfer and imperfect gas effects are beyond the scope of this report, the qualitative trend may be seen by observing the broken line curves on Figures 1 through 5 and on Figure 7. Relatively small percentage changes occur due to heat loss in shock wave velocities and in the pressures at the piston face, and appreciably greater changes occur in the values of the density in the shock layer, the latter being about the same percentage change as the temperatures themselves.

The results of analysis without heat loss (Section III.1.a) appear to be applicable (assuming no friction or viscosity) at the lowest Mach numbers, and the stagnation temperature analysis (Section III.1.b) appears to be qualitatively correct at medium to moderately high Mach numbers.

The physical actions described to this point are applicable whether the tube is open or closed, but are limited to the condition that the shock wave must not have reached the end of the tube. Until that happens the air at the tube-end is undisturbed and the presence or absence of a closure on the end of the tube can make no difference.

When the shock wave reaches the closed end of the tube, the air in the shock layer comes to rest against the tube end. This air previously moved at piston velocity, and the air from that portion of the shock layer which has not yet been stopped still flows into the stopped portion with piston velocity, and the boundary between the stopped portion and the moving portion is the reflected shock wave. This shock wave moves back toward the piston at a speed determined by the rate of accumulation of air at the closed tube end, at the density in that region resulting from bringing the air to rest through the reflecting shock. The temperature and pressure of the stopped air result from the same process.

The similarity between the physical cases (1) when the piston is driving a shock wave before it down a long tube without reflection, as previously described, and (2) when the reflected shock wave is being driven back by a closed end on the tube, may be seen by a shift of reference axes. If, in case (1), the reference axes are anchored in the piston and the observer is there, air is seen flowing toward the piston, coming to rest

against the piston, and accumulating in front of the piston as the process continues. This process causes the shock wave - appearing as a sharp boundary between the in-rushing and the stopped air - to move away from the piston as the air continues to accumulate. Now, to see case (2), the reference axes are anchored in the end of the tube. It is equivalent to the piston in the former case, and the observer is there. Now, air approaches through the tube at piston velocity, arrives at the tube end at the instant of shock wave arrival, comes to rest against the tube end, continues to arrive at piston velocity, accumulates in a layer which grows steadily, forming a discontinuity between the moving air and the suddenly stopped air. This discontinuity is the reflected shock wave. It increases its distance from the closed end of the tube by a physical mechanism which is identical to that of the piston driving the original shock wave. Just as the equations for the conditions across a normal shock apply for the initial piston-driven shock wave, they apply also for the reflected shock wave which must appear in order to preserve the condition that the gas adjacent to the closed end is at rest.

Reflected shock effects may be very strong because the air undergoes two jumps of temperature and pressure for each cycle of reflection, one when the original shock reaches the closed end of the tube and generates the reflected shock and another when the reflected shock reaches the piston and regenerates re-reflection, and the quantities multiply at each jump. At high Mach numbers these ratios are large; such intense changes of temperature and pressure may occur that even the first reflected wave is destructive.

If the tube is short, reflected waves may be especially troublesome because the reflections between the piston and the tube end may pass back and forth so quickly as to produce explosive results, and yet by considering a limited open capacity of the tube relatively little work is done against the piston to brake its motion because the distance traveled is small. For practical use of reflected waves, therefore, the tubes should be long and the vehicle speeds slow.

Pressure, temperature, and density rise discontinuously each time the reflected shock wave arrives at the piston. Expressions (31), (32), and (33) show the strong dependence of these jumps on the velocity of the shock wave, M_W , which depends in turn on the piston velocity, M_P . Figure 9 shows that a piston moving at low Mach number may experience tolerable increases of drag coefficient even after several cycles of reflection, but a piston moving even at the moderate piston Mach number of 4.00 would experience excessive drag pressures at the arrival of the first reflected wave. The drag coefficient rises abruptly at that time from a value of 2.58 to a value of 2170. The ratios of increase for the various quantities may be determined from expressions (31), (32), (33), (34), and (35) by inspection, when used with expressions (7) and (14).

In real air confined within a tube the effects of viscosity cannot be ignored. The shock layer ahead of a perfect piston rubs with piston velocity along the walls of the tube; shearing forces exist in the fluid along the walls which cause a drag reaction at the piston; heating occurs as the air in the boundary layer is sheared; and the homogeneous condition of the shock layer no longer exists. Temperature and density gradients and circulation are present.

do not change as the tube is traversed. On the other hand, viscous effects depend on the presence of a shock layer between the piston and the shock wave, moving at piston velocity, and this does not exist at the first instant of entering a tube, but starts growing at once at the approximate rates indicated in analyses III.2.b and III.3.b.

In the same respect that the effects of gas imperfections may be treated qualitatively as temperature reductions from an otherwise perfect gas system, the effects of friction may be considered as temperature gains, the heat coming from mechanical work against viscous forces, and producing effects opposite to those described previously. That is, as temperature rises in the shock layer due to skin friction, the expectable results move in the direction from the dash lines in Figures 1 through 5, 7, and 10 toward the solid lines and beyond. Density decreases, the shock wave accelerates, pressure at the piston rises, and temperature rises again due to the pressure increase, and so on. The basis of the analysis becomes lost completely if the temperature rise due to skin friction becomes predominantly large.

The analyses of viscous effects, Sections III.2.a, III.2.b, and III.3.b, are necessarily simplifications in view of the complexities of the real case. The temperature rise indicated by the analysis is an average based on complete mixing, and this would not occur. The temperatures would be greater toward the walls and toward the piston, the former because it is

the location of the viscous shearing and the latter because it is the location of air which has been subjected to shearing for the longest time. Heat transfer to the tube would occur at a rate not conveniently analyzed. The air adjacent to the walls would be dragged by the walls toward the piston. With a perfect piston this air would then circulate forward again through the center of the tube (the only available region), accomplishing an undetermined degree of mixing. The air which is heated the most by friction, that which has been in the boundary layer the longest time, would arrive continuously at the piston from the front. With a perfect piston it would arrive at the wall around the circumference of the piston and would then flow radially inward across its face before moving away from the piston upstream. This action would generate a pressure rise due to impact and re-acceleration forwardly and would continuously subject the piston face to the highest temperatures in the system. Any real hypersonic application of a test vehicle in a tube approximating the action of a perfect piston would have to employ means of forcing the very hot viscous boundary layer through the tube walls as it forms, in that way protecting the vehicle from excessive temperatures.

In a long tube the drag due to skin friction with a perfect piston may exceed the greatest amount expected from shock action. In a ten-foot diameter tube, at a piston Mach number of 4.0, at standard sea level temperature, the friction drag coefficient may be expected to exceed the shock drag coefficient after about .98 second, or in 4380 feet of piston travel. To keep the shock from reaching the end of the tube, its length would have to be about 5500 feet. At Mach 8.0, the corresponding figures are .64

second, 5750 feet of piston travel, and 7600 feet of tube length. At subsonic piston Mach numbers, the length of tube required to keep the shock from emerging or reflecting is relatively long. At Mach 0.8, the frictional drag exceeds the shock drag after 3.32 seconds, in 2960 feet of piston travel, in an overall tube length of 5800 feet. In a tube of half the diameter (5 feet) these times and distances would all be cut in half.

At subsonic speed, since the pressures and temperatures are tolerable, reflected waves could be used to increase drag and shorten tube lengths.

At the higher Mach numbers the temperature rise due to friction is likely to predominate over the temperature rise due to shock. At a piston Mach number of 4.0, at the standard sea level temperature of 59°F, the temperature in the shock layer is 2540°F. The average temperature in the shock layer will rise 2540°F again after 1.46 seconds, while the piston traverses 6540 feet of tube. At Mach 8.0 the corresponding figures are 8440°F in the shock layer, increasing by this same amount due to friction after .82 second, in 7320 feet of piston travel. If the tube were 5 feet in diameter instead of 10 feet, these times and distances would be halved.

Even though the accuracy of these numbers may be poor because of the necessary simplifications previously described, it may be seen that the temperature problem, including the effects of friction, is of serious proportions. The use of a high degree of tube evacuation to reduce the heat transfer rate to the test vehicle is of little value here because piston action would preferably be avoided when the tube is evacuated, as is consistent to obtain low drag. On the other hand the braking function, fully

employed, calls for a maximum both of air density and piston action. A high rate of aerodynamic heating is inherently associated with large braking forces.

A perfect piston in a perfect tube without leakage in either part has been assumed in the preceding discussion. In the real case there would be some escape of air from the shock layer, either as a consequence of imperfect mechanical fit of the body in the tube or by design.

Leakage out of the shock layer reduces the rate of mass accumulation ahead of the piston, in that way reduces the velocity of the normal shock wave running ahead of the piston, and correspondingly reduces the magnitude of the jump in pressure, temperature, and density through the shock wave, causing reductions in these quantities at the front of the body.

When air is lost from the shock layer at the same rate at which it is received, the lower limit of piston action has been reached, and the shock wave velocity equals the piston velocity. If more air is lost from the shock layer the shock no longer stands in front of the body but falls back on the body as an oblique shock wave, and reflects from the tube onto the body, so that the flow is no longer in the piston regime but is in the shock interference regime.

The relative rates of inflow to and outflow from the shock layer determine the degree of piston action. If the shock layer increases in size with time, the shock wave velocity exceeds the piston velocity and relatively increased values of pressure, temperature, and density exist at the front face of the piston. The rate of mass flow from the shock layer

is determined by the total of the outlet cross-sectional area through which air may escape; this consists of the circumferential gap area around the body plus the orifice area in the tube in contact with the shock layer at any instant.

In nearly every case having practical interest the pressure in the shock layer will be sufficiently large relative to the pressure in the escape region (behind the piston or outside the tube) to cause air to escape at local sonic speed in the escape gaps and orifices, permitting convenient analysis. See Section III.3.a.

The dotted lines in Figures 1, 3, and 5 show the lower limit of piston action ($M_w = M_p$) relative to the two cases of the upper limit or perfect piston action previously described. See also expressions (54), (55), and (56), and Figures 12 and 13.

It will be observed from Figure 13 that the maximum allowable escape ratio at which the lower limit of piston action will be achieved becomes essentially constant at hypersonic Mach numbers. From expression (55) it may be seen that the maximum ratio of gap area to tube area is $\sqrt{1/7}$ at infinite piston velocity, and is larger at lower piston velocities, so that the ratio of piston area/tube area for a tube without wall orifices is .622, or the ratio of body diameter to tube diameter is .789. As a practical rule of thumb, then, if one wishes to achieve the regime of high pressures ahead of an object moving through an impervious tube at supersonic speed, this will always be achieved if the body diameter is at least 8/10 of the inside diameter of the tube. Similarly, when an object is propelled from a tube by gases at high pressure, the predominant portion of the total available effect

will be achieved if the body diameter is at least $8/10$ of the tube diameter. It will be seen that the practical gap permissible between the body and the tube wall in these cases is ample for practical applications.

Figure 13 also indicates that the gap ratio A_G/A_T may be as large as 1.0 at Mach 1.0 and that minimum piston action will be achieved. At this gap ratio, if there is no leakage through the tube, the entire cross-sectional area of the tube consists of "gap"; the body cross-sectional area is infinitesimal. This may be interpreted physically: at Mach 1.0, the shock front from a point body must be normal to the tube because all pressure disturbances originate at the body and run forward through the tube at sonic speed, as does the body; and all of the flow which enters the shock from the front escapes past the body through the available gap at sonic speed. This physical picture agrees with the mathematical requirements for the lower limit of piston action, even though one does not ordinarily think of an infinitesimal body behaving like a piston.

When the speed of the infinitesimal body exceeds Mach 1.0 its shock wave becomes oblique, and the flow no longer lies in the piston regime. But if the body gains cross-sectional area as indicated by Figure 13 as it gains speed, it throttles the rate at which mass can escape rearwardly. This causes air to accumulate in the shock layer, the shock is pushed forward and becomes a normal shock, again achieving piston action.

A moving piston advancing into still air is the same as moving air advancing on a stationary piston, or upon a tube end. Just as a completely closed tube behaves as a perfect piston, a partially closed tube end acts as an imperfect piston, or as no piston at all if its gap ratio is excessive.

Just as Figure 13 gives the maximum gap at which piston action is achieved, it also gives the minimum gap at which piston action is avoided. The fundamental quality of piston action (as this term is used in this report) is the ability to drive a normal shock wave through the tube. If piston action is avoided, the ability to drive a normal shock through the tube is avoided. Therefore, Figure 13 also shows the minimum open area at the tube end which will prevent shock wave reflection. For example, at Mach 1.0, a Mach wave will reflect unless $A_G / A_T = 1.0$; that is, the tube must be wide open to avoid reflection. A normal shock advancing at Mach 4.0, from Figure 13, will not reflect if at least 43.5 percent of the tube end area is open; and a normal shock at Mach 20 will not reflect if about 38 percent of the area at the end of the tube is open - within the limitations of the present analysis.

Viscous effects with imperfect pistons are prominent to the same degree that the distance from the piston to the normal shock is large, or in other words, to the same degree that the piston action approaches perfection. To obtain the least viscous effects, then, the flow should be at the lower limit of piston action, and the shock should have fallen back to the piston. To make the shock fall back, vent area distributed along the tube wall is effective. This area adds to the gap area around the piston but only when in contact with the shock layer; if the shock layer is thick the gap area is large and large amounts of mass escape through the walls. The shock layer stabilizes at the body if the gap ratio of the body is as shown in Figure 13, or somewhat in front of the body if the gap ratio of the body is somewhat less than shown in Figure 13. The same vent area in

the wall which shortens the shock layer could be so arranged that the air removed would be the hottest part of the shock layer, the viscous-heated boundary layer.

The reduction of the shock layer depth to a small value at the lower limit of piston action also eliminates any significant amount of heat loss through the walls, so that a perfect gas analysis without heat loss should apply accurately at low supersonic Mach numbers. Then, the pressure, drag, temperature, and density conditions at the front of the body in the tube are the same as those which exist at the same velocity on a flat-faced body of the same diameter in the open air, but of course the body in the tube need not be flat-faced; it may be of any shape whatever.

At the lower limit of piston action, then, the effect of the tube is equivalent to changing the effective form of a body. A slender-nosed body with a drag coefficient of 0.2 in free air acquires a drag coefficient above 1.6 at minimum piston action in a tube, an increase by a factor of more than eight (without the necessity of any mass for drag modulation structure being carried by the body).

The broad pattern of additional effects obtained with better piston action may be seen from the general form of equations (2) and (3) and from Figure 1. At hypersonic speeds, pressures and temperatures are roughly proportional to the square of the shock velocity, and to the square of the piston velocity, and perfect piston action increases shock wave velocity by a factor of about 1.2, as compared to minimum piston action. Thus, perfect piston action increases the effects of minimum piston action by about

44 percent, at hypersonic Mach numbers. Accordingly, the drag of a refined aerodynamic body increases about twelvefold upon entering a close-fitting braking tube at hypersonic speed, to which is added the very large drag rise due to viscosity. And at lower speeds, the relative rise in drag due to shock is greater.

3. Discussion of Practical Aspects

The magnitudes of the physical quantities which are indicated for a hypersonic test vehicle in a tube are impressive. Assume for the sake of discussion that a vehicle enters a 4-foot diameter tube for braking purposes and behaves as a perfect piston at Mach 10.0 for one second. At the end of that time, according to a perfect gas analysis, the shock layer in front of the piston is 2320 feet thick, exerts a pressure of 360,000 pounds per square foot inside the tube, and has a temperature of 15,000°F. Frictional heating adds an additional 43,000°F to the average temperature of the shock layer. This invalidates the basis of the perfect gas analysis.

These numbers lose value for specific purposes, but the over-all impression is valid: the effects are formidable at the higher Mach numbers.

By enclosing a hypersonic test track, two main functions may be served: (1) evacuation to lower aerodynamic drag and (2) action by the tube to increase aerodynamic drag. To accomplish (1) the tube must be large, and to accomplish (2) it must be small relative to the test vehicle. The practical difficulties inherent in such a contrary situation are apparent.

The gas dynamics in the large tube are in the "free" regime, and in the small tube are probably in the piston regime; these regimes have been

studied. But between these two extremes there is need for further definition, particularly regarding the flow behavior with typical rocket bodies which are so long that shock waves reflected from the walls of an enclosing structure of economical size would not pass behind them. Favorable wave interference effects (reference [5]) probably cannot be utilized because these require a body form which tapers to the rear, unlike rocket vehicle design. Yet, unfavorable wave interference effects should be avoided if possible.

At high Mach numbers the surge of intense pressure and temperature along the tube will increase the problems of keeping the tube airtight for evacuation. The greatest problem of the vehicle will be high temperature, so very high that the use of an enclosed high-speed track for high temperature research is naturally suggested.

The portion of the temperature due to skin friction is avoidable by the use of sufficient venting of the tube to operate at the lower limit of piston action, and with enough gap between the vehicle and the walls to allow the passage of any hot boundary layer which does not escape through the tube walls. Ablation materials used to protect the vehicle also need space through which to pass rearwardly.

At the higher Mach numbers a plasma sheath will enclose the test vehicle, adding greatly to the problems of radio transmission from the inside of the tube.

Yet a need exists for a new method of vehicle braking. Even on comparatively slow test tracks already in operation, the limitations of other braking systems have been reached. Water braking, accomplished by scooping

up water, has proved ineffective at the higher speeds for several reasons: the water does not enter and flow through the scoops but bursts into a cloud of spray; the mass of the scoop system carried by the sled absorbs energy during acceleration and limits the maximum speed otherwise attainable; and the braking reaction is applied eccentrically to the sled causing extraneous loads and weight in the structure and at the slippers. Since the water supply is limited birds are attracted to the test track and by their presence interfere with the testing and cause damage to the sleds. Braking by picking up mass other than water has practical limitations; the material does not transmit stresses quickly enough to permit the entire mass to be accelerated. For example, unattached nylon ropes draped loosely across the track with their free ends extending in the direction of sled motion are reportedly severed by the sled at the point of contact without being moved otherwise. The use of a long tube for braking does not have any of these particular disadvantages but it does have others.

Since the effect of the tube depends upon the relative size of the body passing through it, an enclosed track has considerably less versatility than an open track. It also involves extra cost due to the enclosing structure, the evacuation tanks the pumps, the power to operate the pumps and the loss of test time while evacuating.

The non-braked portion of an evacuated tube could attain versatility (at a high cost on all the counts just mentioned) by being as large as required for the largest test vehicle contemplated. But such a tube would not serve for braking. Neither a very large nor a very small portion

of an evacuated tube can perform the function of the other, because test vehicles must fit the tube within prescribed limits. Either test planners would have to accomplish the correct velocities, times and distances for the various phases of tests run in a tube having different diameters and different evacuation in different segments or some sort of variable construction would be needed.

Not only the test vehicle but boosters including extra stages have to be considered. The braking of a detached booster following the test vehicle through a braking tube could be a difficult problem.

If the entire length of an enclosed evacuated test track were constructed at one moderate diameter, the effective diameter of the test body would have to be variable. This direction of study would contemplate the use of a body as small as needed to avoid minimum piston action, with the intention of tolerating the reflection of oblique shock waves from the tube during the non-braked portion of the run, and the use of an expanding construction, perhaps resembling aircraft engine cowl flaps, to change the modus operandi of the vehicle from the low drag regime to the high drag piston regime. The same flaps could be used to modulate the drag, to hold the deceleration at a permissible value according to a particular program. In this constant diameter tube the air density could be different in different segments and the tube wall venting could be adjustable for desired effects.

The function of the braking tube, taken by itself, can be accomplished in a non-evacuated tube. Such a tube could conceivably be designed with adjustable diameter, for example, by means of a flexible wrap-around

structure. But this does not sound promising for use at moderate to high Mach numbers in view of the high pressures which occur even at the lower limit of piston action.

To obtain braking action in an atmospheric braking tube of constant area, with various sizes of test vehicles, it might be possible for a lightweight piston of tube-fitting size and shape to be picked up by the test vehicle shortly before it enters the braking tube. To reduce the relative velocity between vehicle and piston to acceptable values, the special piston body would be rocket accelerated ahead of the approaching test vehicle, timed to meet without excessive impact before the combination entered the tube.

To avoid excessive pressures within the tube, and in some cases to control the rate of deceleration of the test vehicle, a tube could employ large pressure-actuated relief valves, such as narrow chord hinged doors, having small inertia. At the lower Mach numbers where temperatures are not excessive and very large pressures may be obtained by reflection if necessary, such a construction appears especially suitable. At any Mach number, the design of gaps around the body and venting in the tube would be governed first by the necessity of avoiding excessive temperatures, after which braking pressures would still be adequate, and drag modulation could be controlled by valving off pressures in one way or another.

In view of these considerations a small atmospheric tube over a monorail track for braking sleds having a standardized frontal area from about Mach 3.0 down to zero speed appears feasible. At higher Mach numbers the aerodynamic drag in the open air is often sufficient to produce

as much deceleration as the payload will tolerate, and the ability to achieve effective braking in a tube right down to zero velocity would eliminate entirely the need for water braking. In a destruction test, running off the end of the track at full speed, the tube venting would all be opened wide, and for the greatest possible braking the venting and the tube end would be closed and reflected shocks would be used.

It must be understood, of course, that precision programming of a braking tube would require consideration of the effects of piston acceleration and deceleration on pressures and temperatures, which are beyond the scope of the present report. These effects can be significant. In perfect piston action after one second in a tube at 60°F at Mach 3.0 the shock wave is 900 feet ahead of the piston, so that a reduction of speed at the piston cannot instantly change the speed of the shock wave. A finite time is required for pressure adjustment throughout the shock layer, even at the elevated temperature and high-sound velocity in that layer.

V. CONCLUSIONS

1. Ample pressure is available for braking purposes.
2. Drag coefficients at high Mach numbers are typically 2.40 for a body fitting very closely in the tube and 1.66 (the same as a flat-faced body in free air) for a body having a diameter 0.8 of the tube diameter.
3. Drag coefficients are relatively higher at the lower Mach numbers, with values of 4.0 near Mach 1.0 and 20.0 at Mach 0.1 for close-fitting bodies.

4. Typically an aerodynamically clean body increases drag about twelvefold upon entering a close-fitting tube at high Mach numbers, and fiftyfold at Mach 0.5.
5. To achieve the bulk of the effect of the tube in increasing braking pressures, the body diameter should not be less than 0.8 of the diameter of the tube at high Mach numbers, nor less than 0.65 of the diameter of the tube at Mach 2.0.
6. Shock waves reflected from the closed end of the tube produce very large pressures and temperatures, except at the lowest Mach numbers.
7. To prevent shock wave reflection from the end of an impervious tube ahead of a very close-fitting body, about 40 percent of the cross-sectional area of the tube end must be open at a body speed of Mach 20.0 and about 45 percent must be open at Mach 4.0.
8. Very high temperatures may be expected on a close-fitting test vehicle at high Mach numbers.
9. Drag and temperature due to viscosity predominate over drag and temperature due to shock in long tubes traversed by close-fitting bodies at high Mach numbers.
10. Practical problems exist in making a tube fit various sizes of test bodies properly for both the low drag and braking functions.
11. A small-sectioned atmospheric braking tube for a monorail track appears to be feasible.
12. Quantitative values of pressure, temperature, and density ratios are presented in equations, charts, and tables.

TABLE I
PERFECT PISTON ACTION

Perfect Gas

$$\gamma = 1.4$$

No Heat Loss

$$\frac{A_G}{A_T} = 0$$

M_W	M_P	M_S	$\frac{P_2}{P_1}$	$\frac{T_2}{T_1}$	$\frac{P_2}{P_1}$
1.0	0	1.000	1.000	1.000	1.000
1.2	.306	.894	1.513	1.128	1.341
1.4	.571	.829	2.120	1.255	1.690
1.7	.926	.774	3.204	1.459	2.198
2.0	1.250	.750	4.500	1.687	2.668
2.4	1.653	.747	6.551	2.040	3.213
3.0	2.222	.778	10.33	2.679	3.856
4.0	3.125	.875	18.49	4.046	4.571
5.0	3.998	1.002	29.00	5.800	4.990
6.0	4.861	1.139	41.82	7.941	5.268
8.0	6.560	1.440	74.50	13.38	5.555
10.0	8.250	1.750	116.4	20.39	5.714
12.0	9.931	2.069	167.8	28.94	5.799
15.0	12.444	2.556	262.2	44.69	5.868
18.0	14.954	3.046	377.7	63.94	5.909
21.0	17.460	3.540	514.1	86.65	5.932
25.0	20.799	4.201	729.0	122.5	5.951

TABLE II
IMPERFECT PISTON ACTION

Perfect Gas

$\gamma = 1.4$

No Heat Loss

M_W	$\frac{A_G}{A_T} = 0.1$		$\frac{A_G}{A_T} = 0.2$		$\frac{A_G}{A_T} = 0.3$		$\frac{A_G}{A_T} = 0.4$	
	M_P	M_S	M_P	M_S	M_P	M_S	M_P	M_S
0.8	(-.283)	(1.083)	(-.190)	(.990)	(-.098)	(.898)	(-.006)	(.806)
0.9	(-.079)	(.979)	.017	.883	.113	.787	.210	.690
1.0	.100	.900	.200	.800	.300	.700	.400	.600
1.3	.551	.749	.660	.640	.770	.530	.879	.421
1.9	1.272	.628	1.398	.502	1.525	.375	1.652	.248
2.5	1.896	.604	2.043	.457	2.189	.311	2.335	.165
3.5	2.861	.639	3.043	.457	3.225	.275	3.407	.093
5.0	4.241	.759	4.482	.518	4.727	.273	4.963	.037
10.0	8.701	1.299	9.153	.847	9.604	.396	(10.056)	(-.056)
16.0	13.994	2.006	14.706	1.294	15.418	.582		
24.0	21.028	2.972	22.091	1.909	23.153	.847		

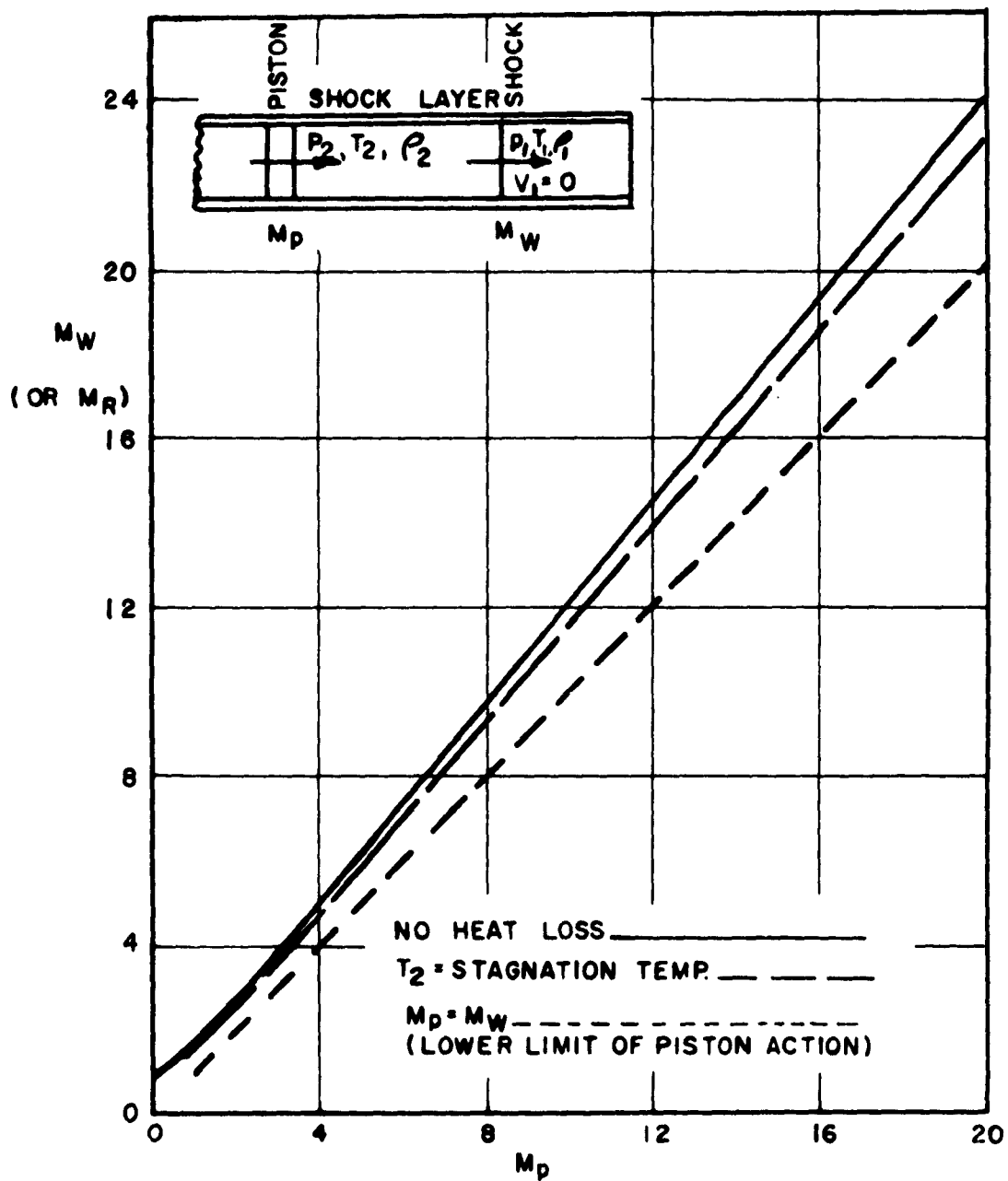


Figure 1a. Normal Shock Wave Velocity Versus Piston Velocity
 $M_p = 0$ to $M_p = 20$

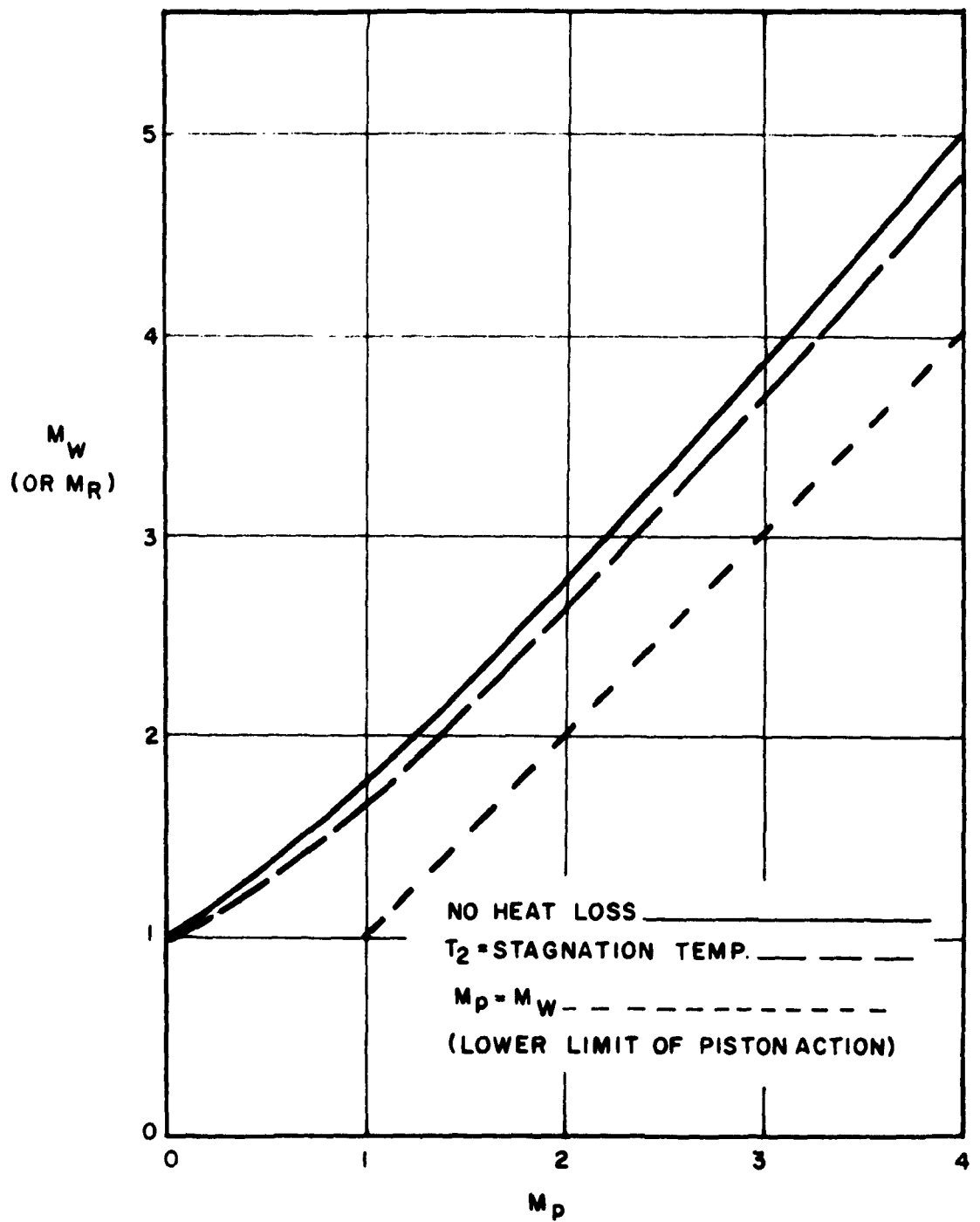


Figure 1b. Normal Shock Wave Velocity Versus Piston Velocity
 $M = 0$ to $M = 4.0$

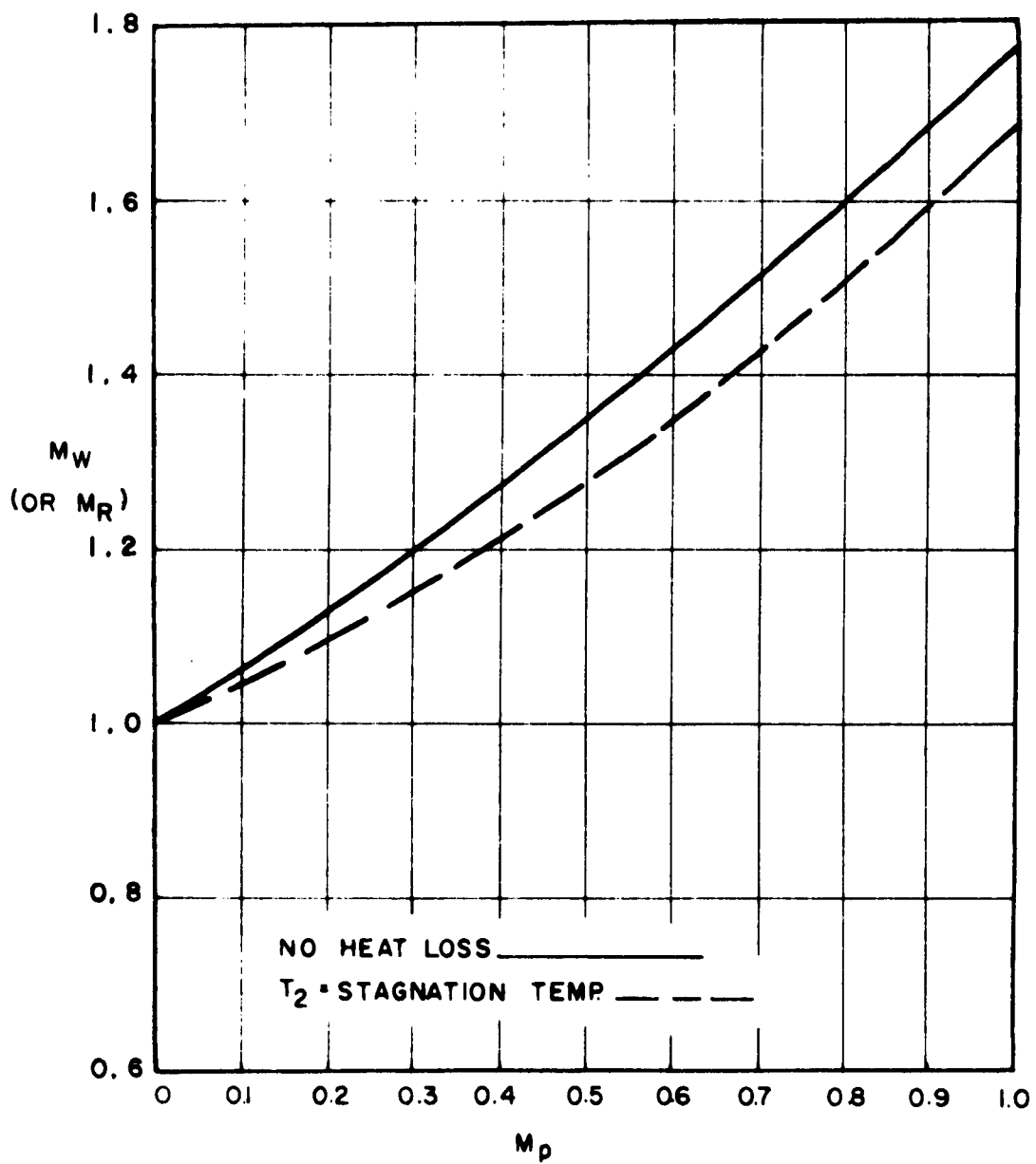


Figure 1c . Normal Shock Wave Velocity Versus Piston Velocity
 $M_p = 0$ to $M_p = 1.0$

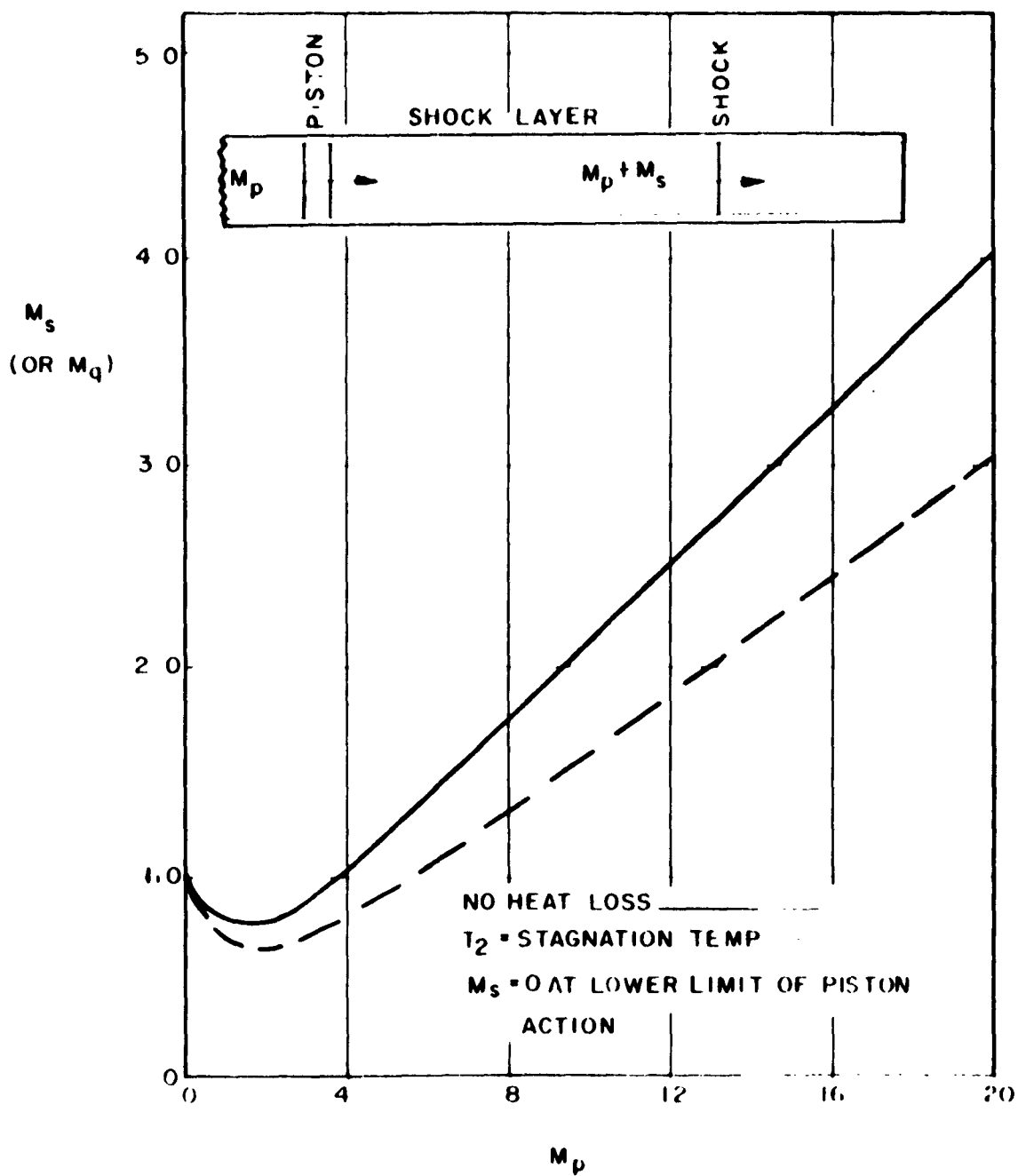


Figure 2. Additional Normal Shock Velocity Versus Piston Velocity

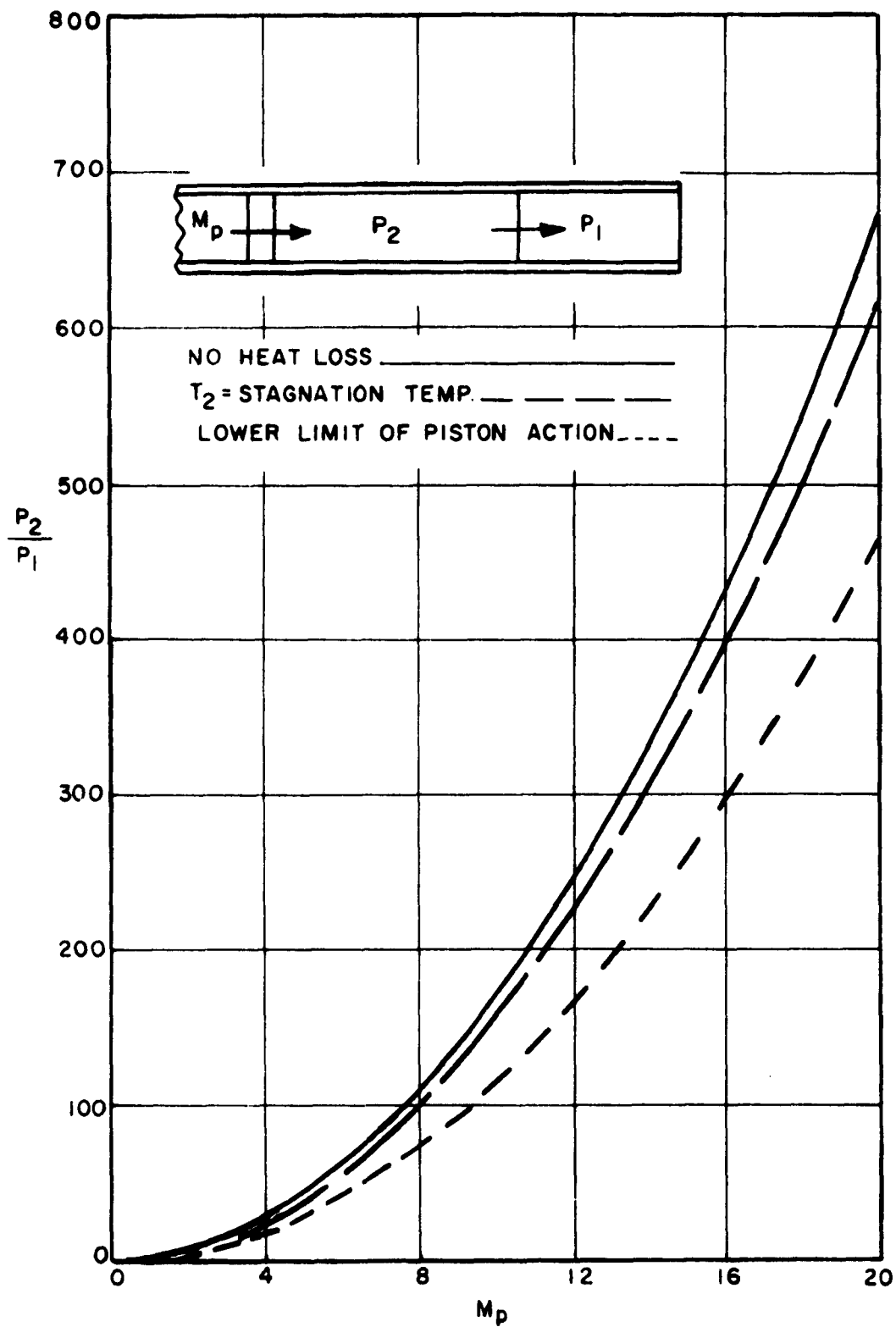


Figure 3a. Pressure Ratio Versus Piston Velocity $M_p = 0$ to $M_p = 20$

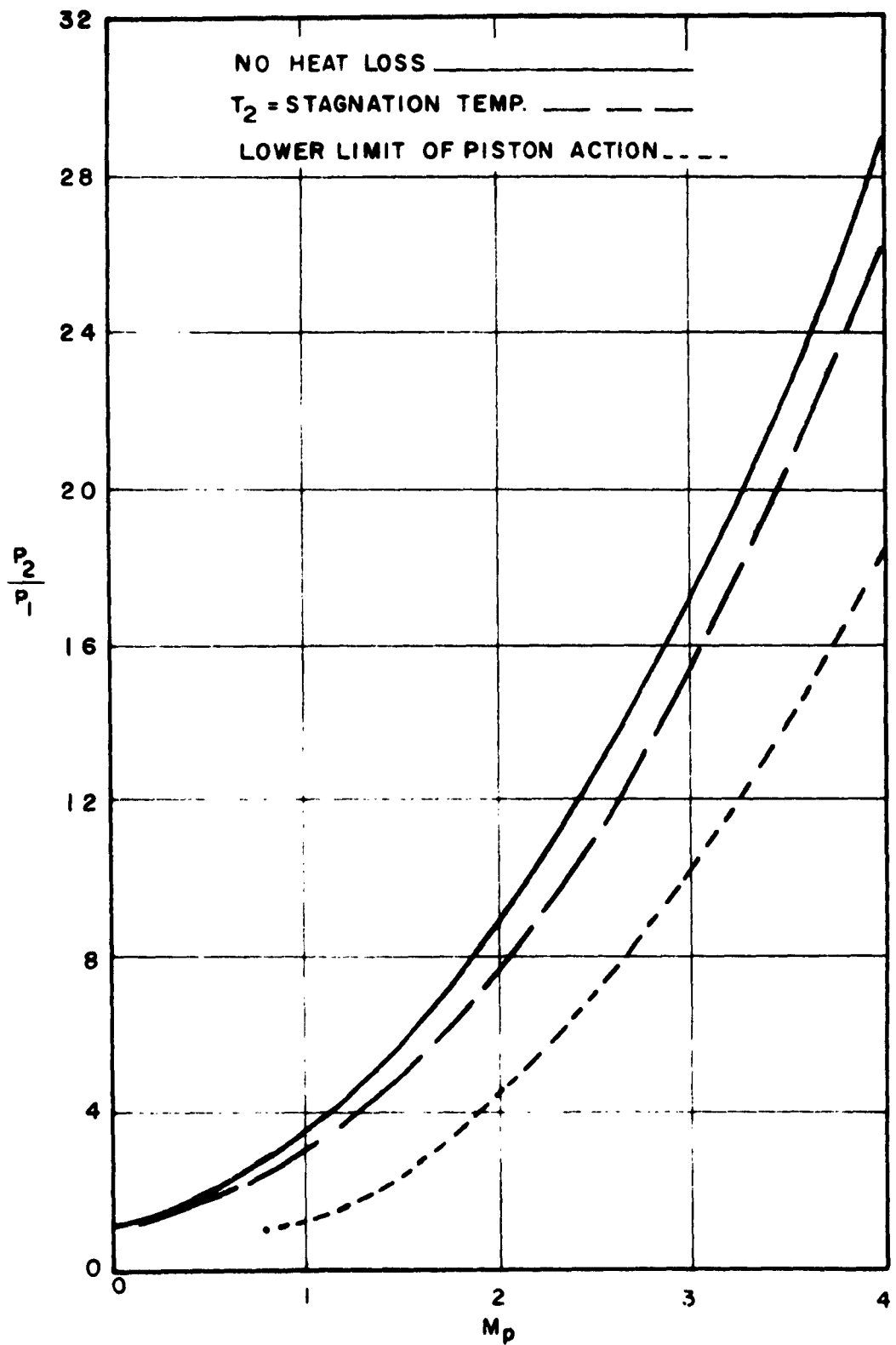


Figure 3b. Pressure Rate Versus Piston Velocity $M_p = 0$ to $M_p = 4.0$

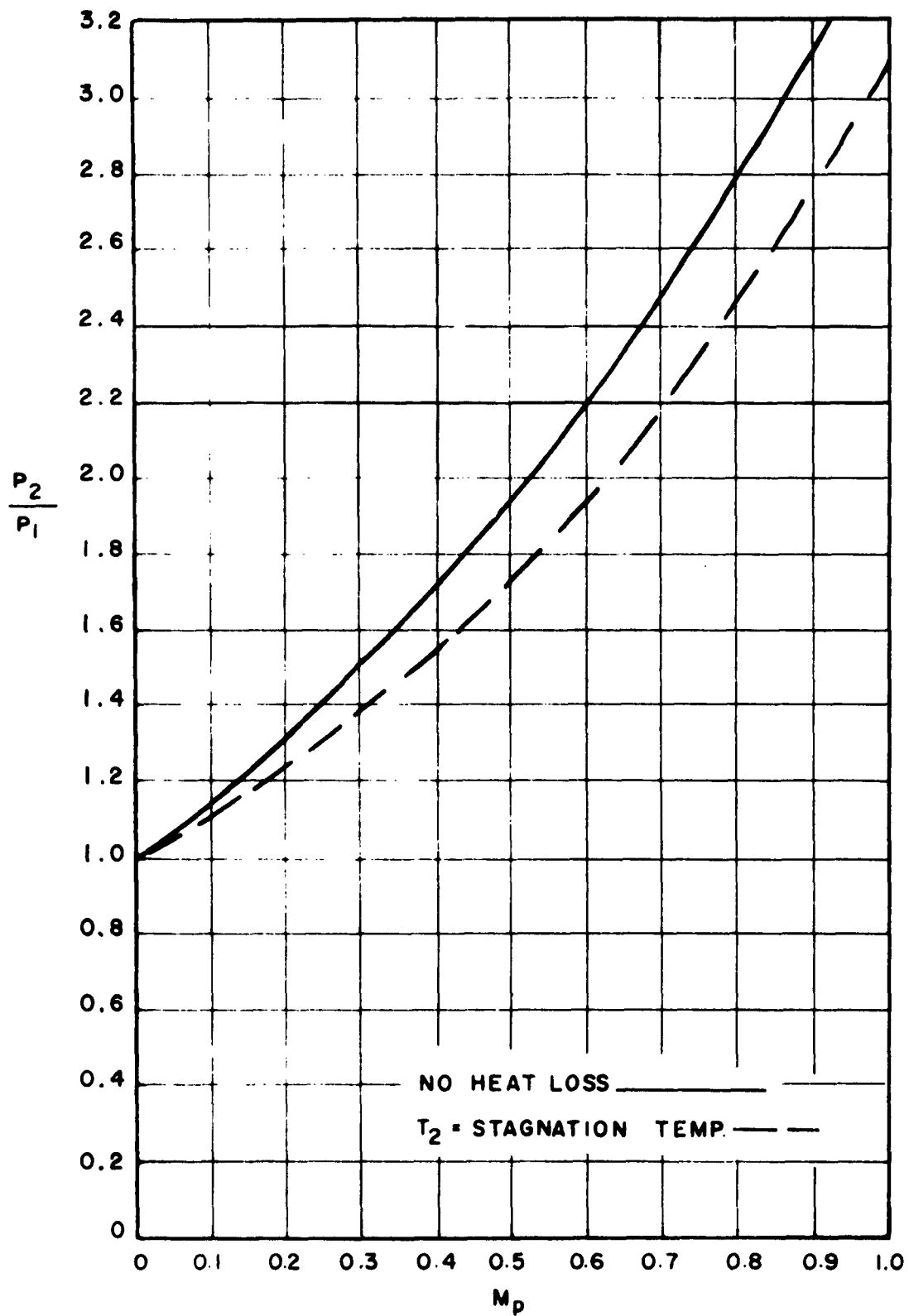


Figure 3c. Pressure Ratio Versus Piston Velocity $M_p = 0$ to $M_p = 1.0$

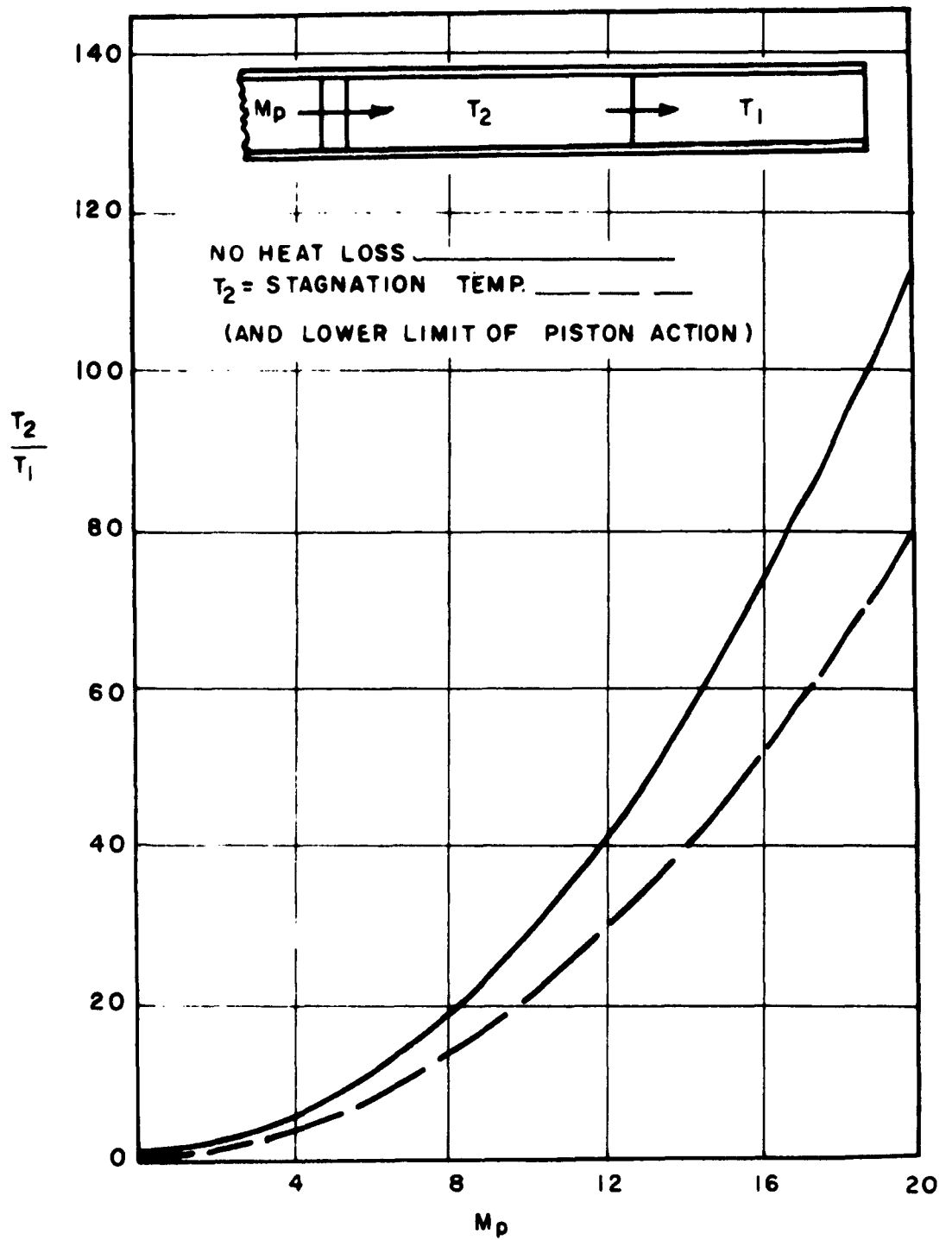


Figure 4a. Temperature Ratio Versus Piston Velocity $M_p=0$ to $M_p=20$

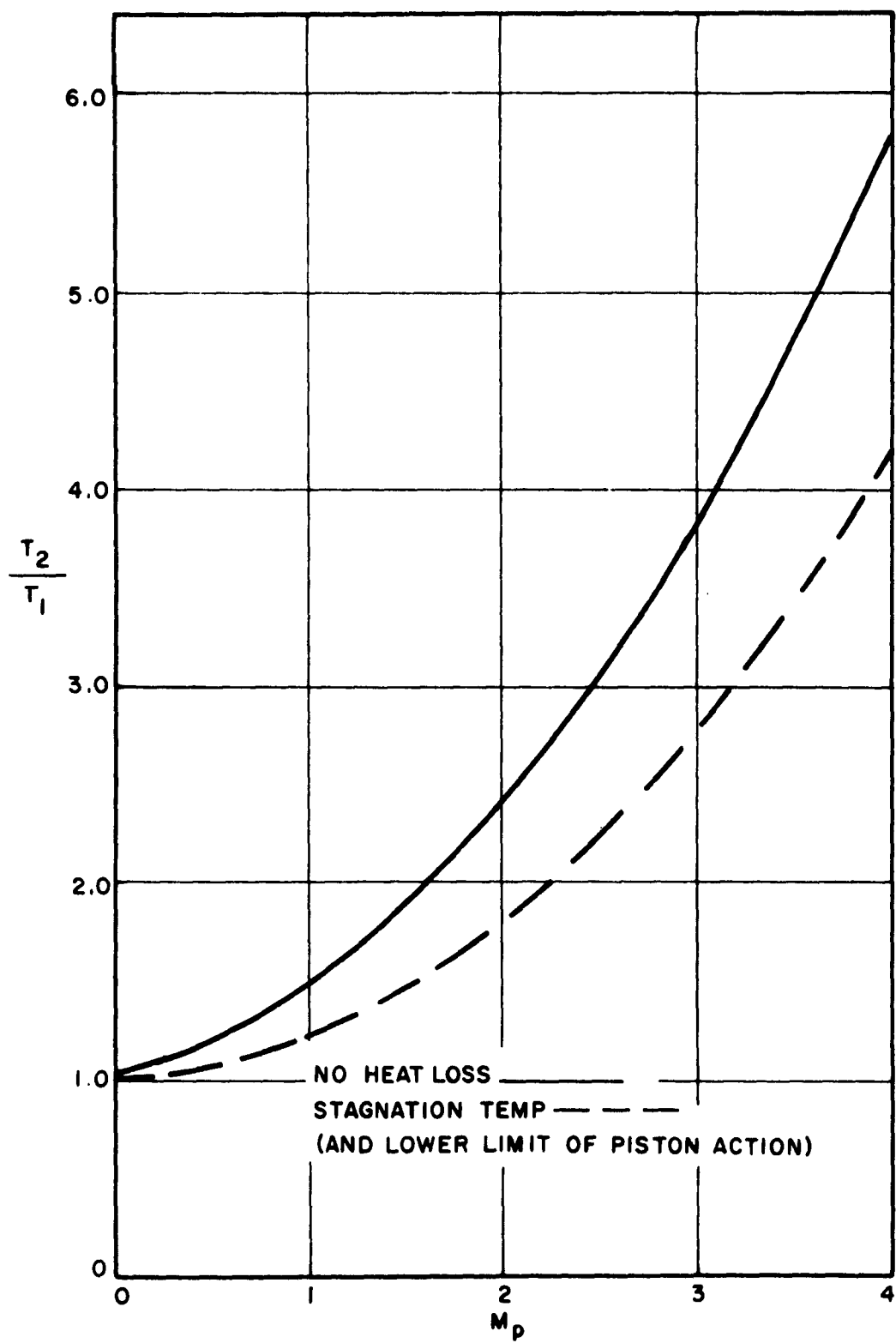


Figure 4b. Temperature Ratio Versus Piston Velocity $M_p=0$ to $M_p=4.0$

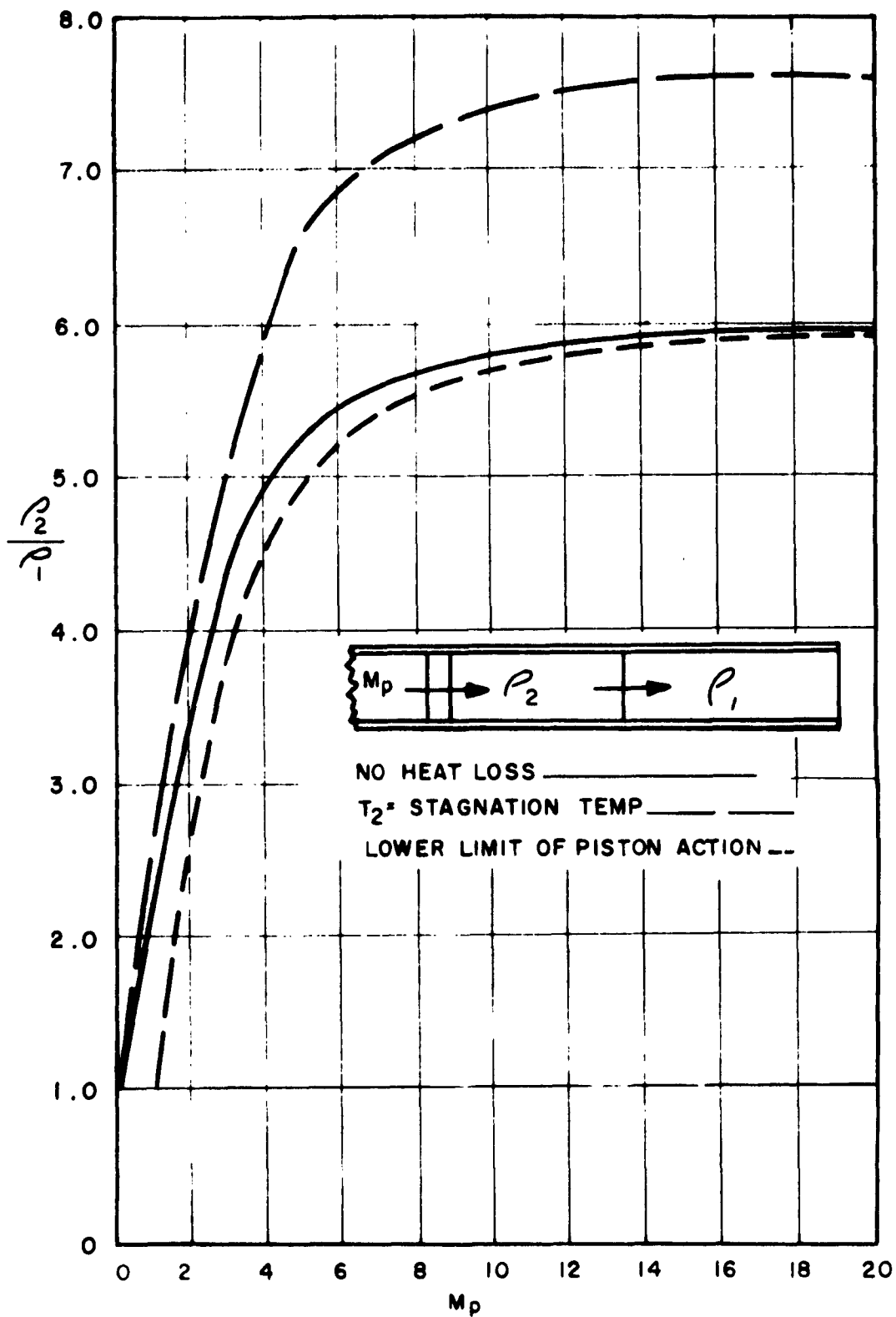


Figure 5. Density Versus Piston Velocity

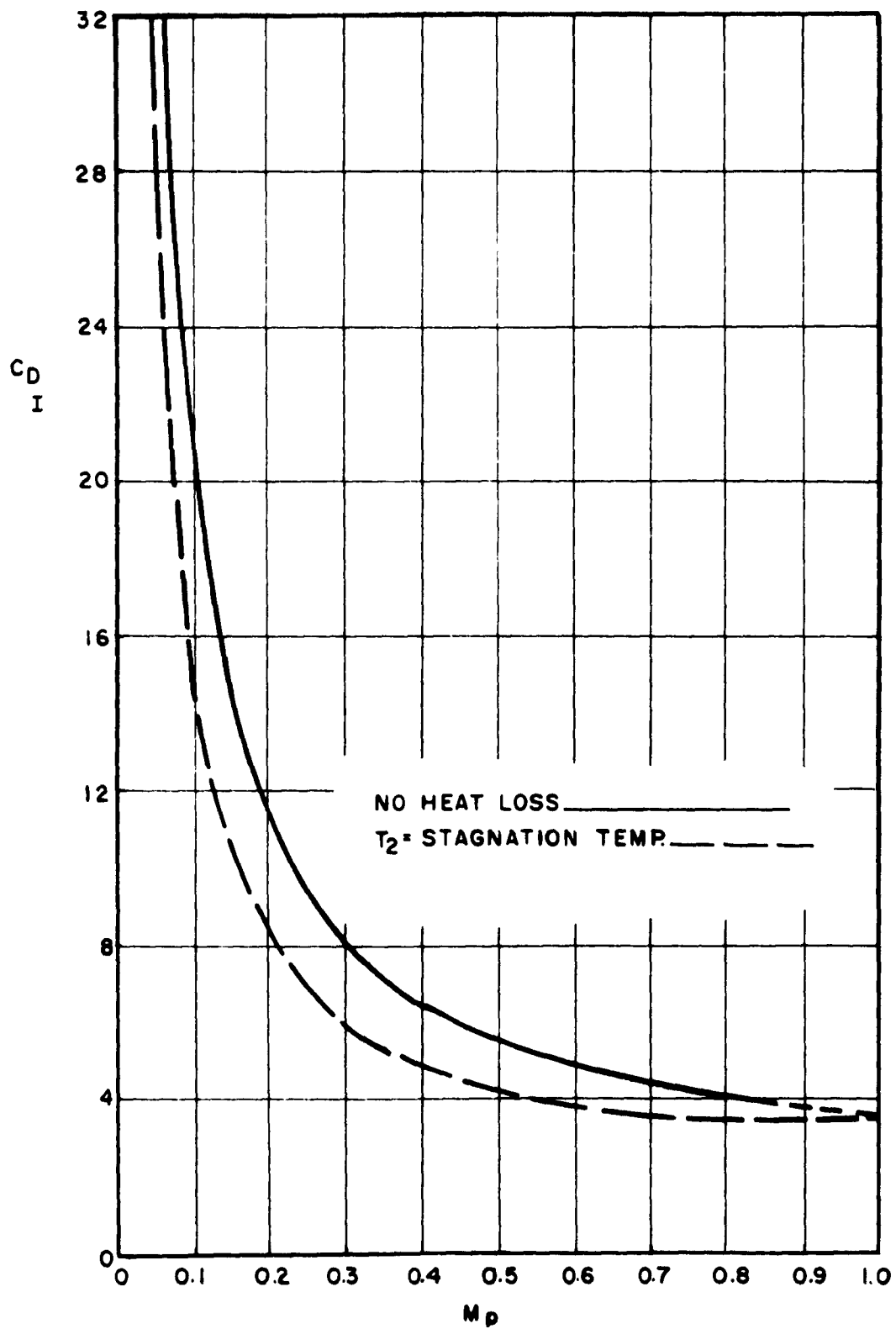


Figure 6. Drag Coefficient Versus Piston Velocity

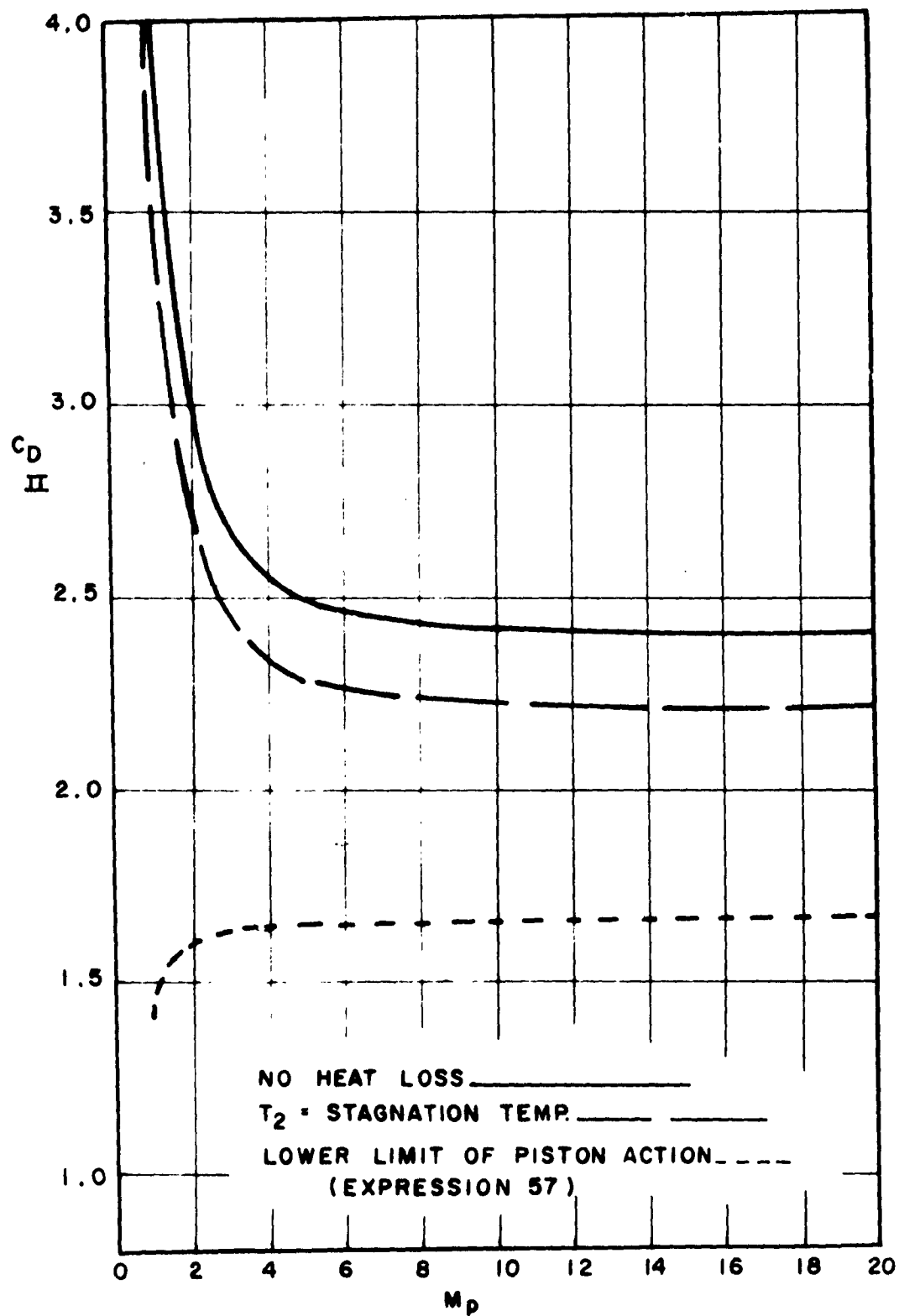
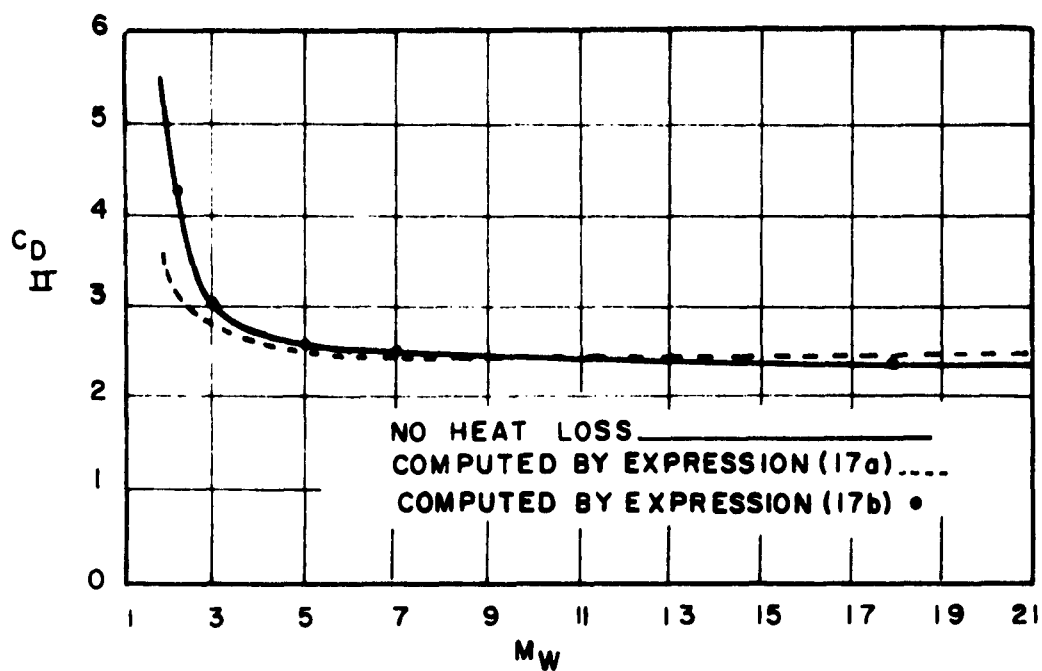
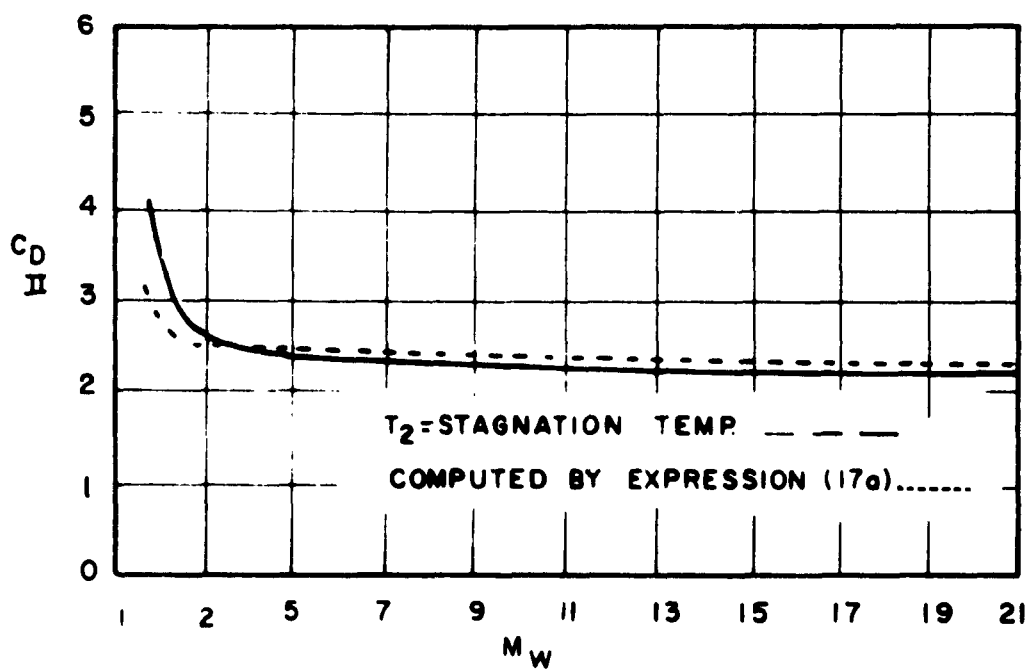


Figure 7. Drag Coefficient Versus Piston Velocity



----- COMPUTED BY RATE
OF CHANGE OF MOMENTUM ASSUMING PLASTIC
PICKUP OF MASS (18)



DRAG COEFFICIENT VS. SHOCK-WAVE VELOCITY
Figure 8. Drag Coefficient Versus Shock Wave Velocity

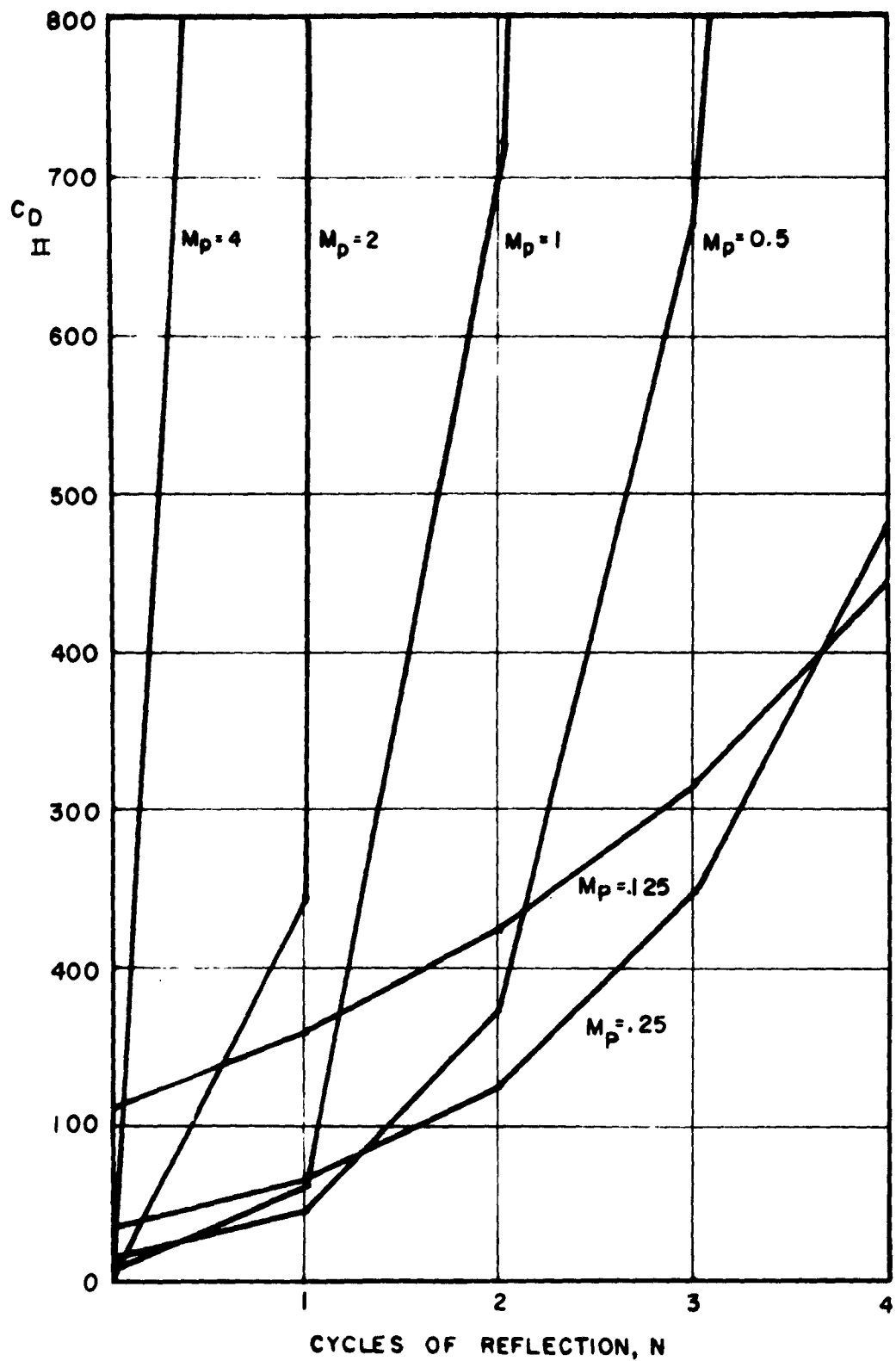


Figure 9. Drag Coefficient Versus Cycles of Wave Reflection

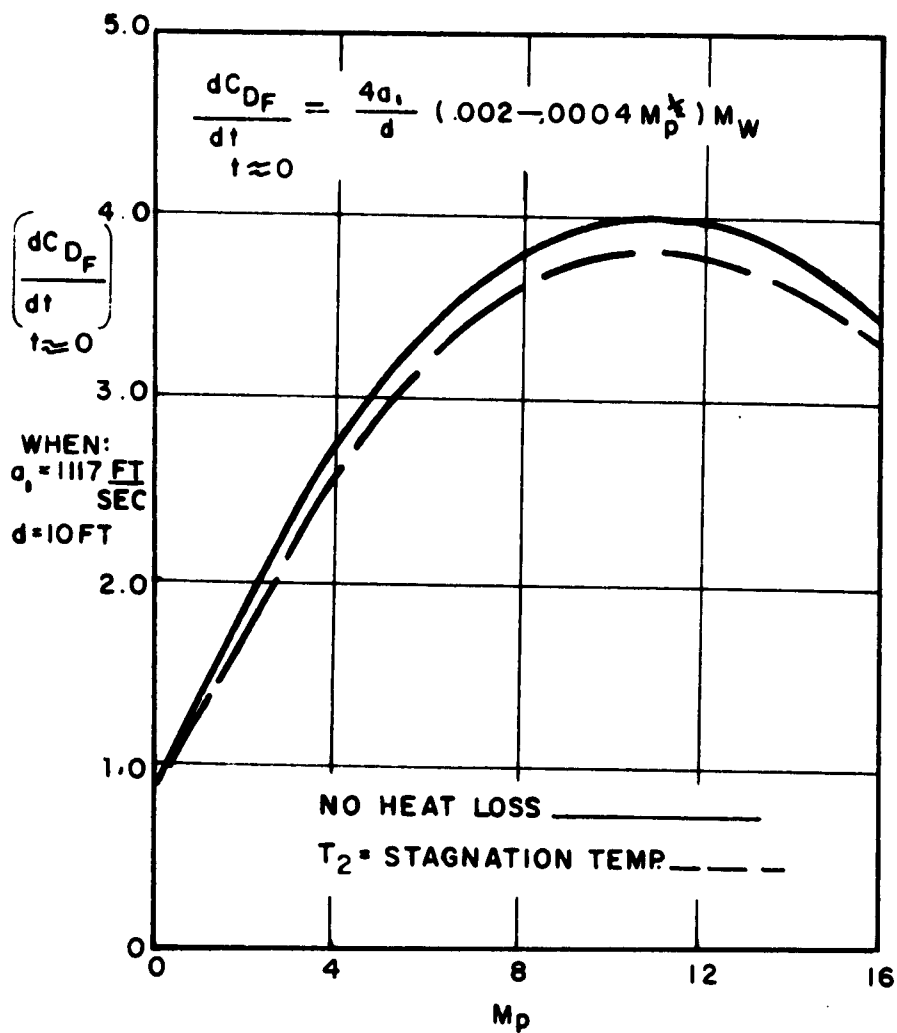


Figure 10. Frictional Drag Rise Rate Versus Piston Velocity

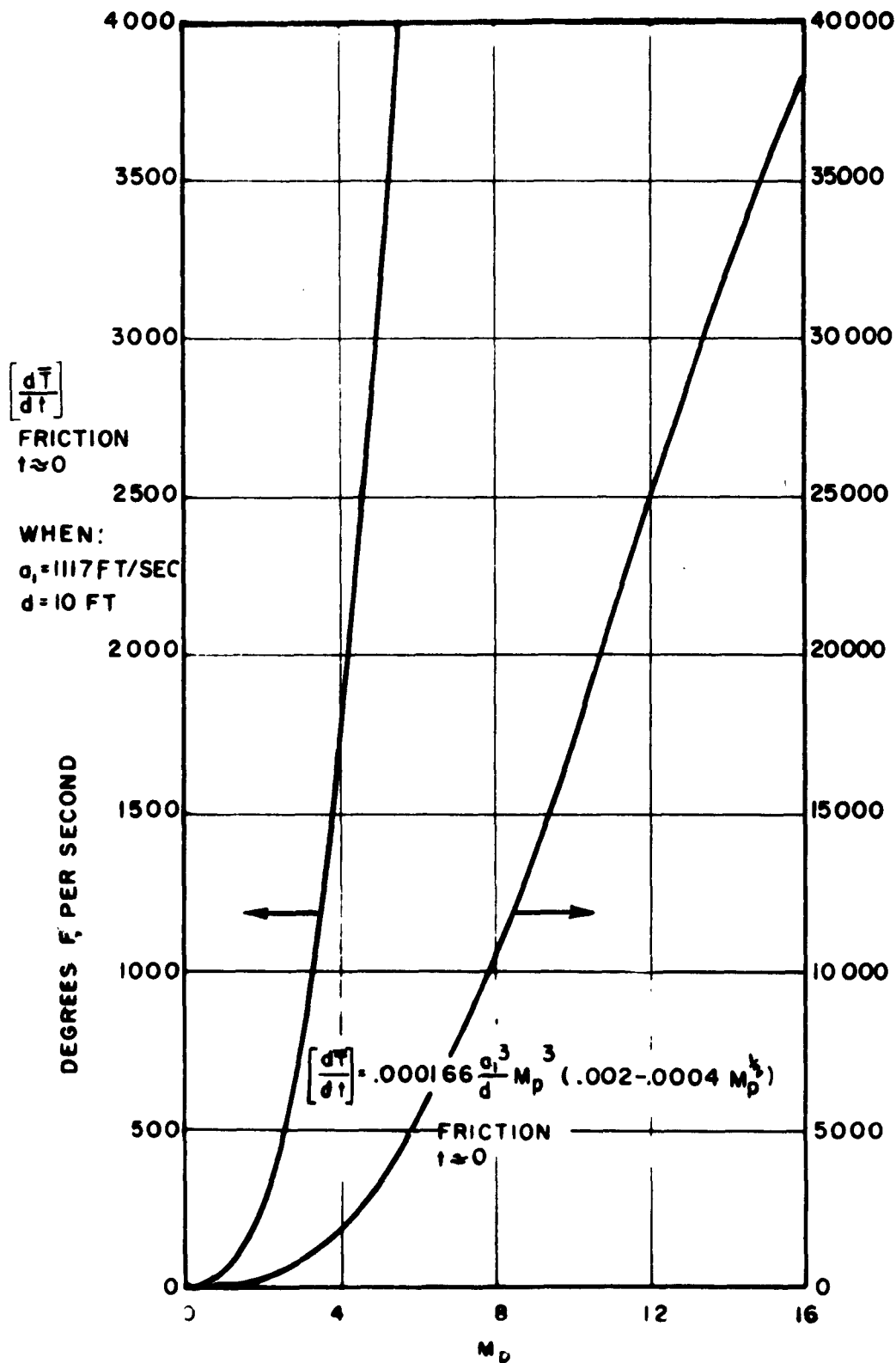


Figure 11. Frictional Temperature Rise Rate Versus Piston Velocity

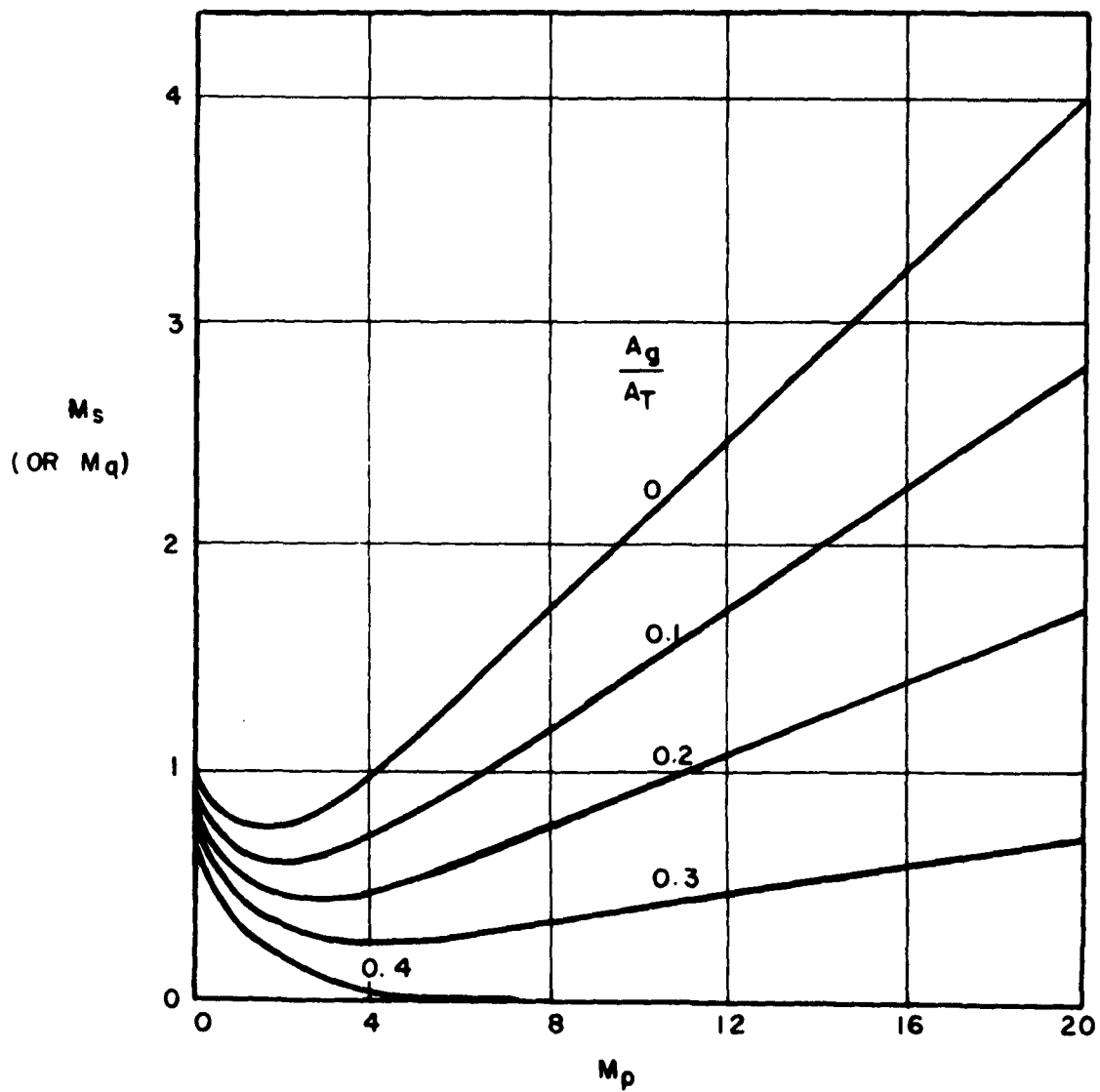


Figure 12. Additional Normal Shock Velocity Versus Velocity of an Imperfect Piston

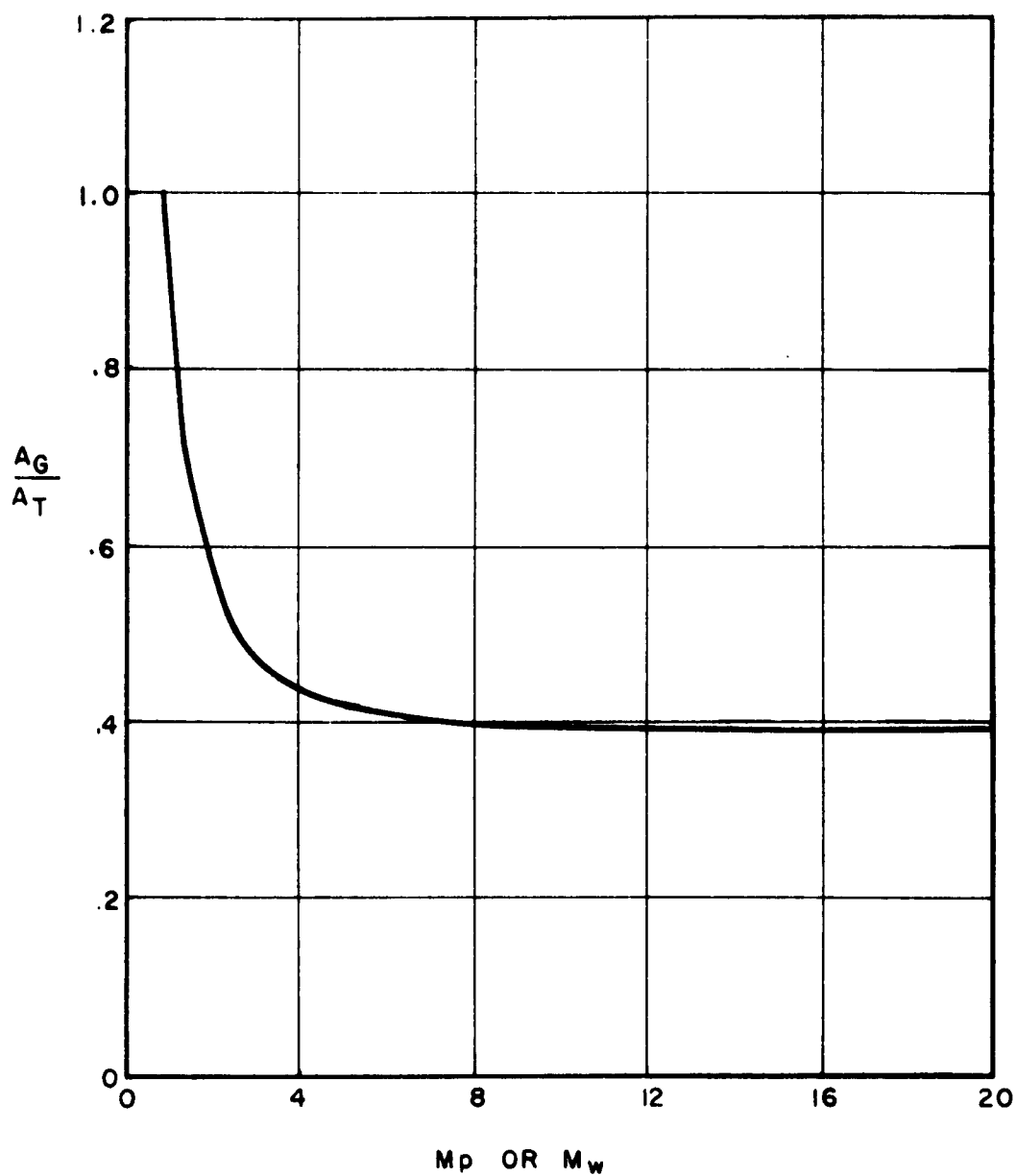


Figure 13. Orifice Area Ratio Versus Piston Velocity at the Lower Limit of Piston Action

REFERENCES

- [1] Ames Research Staff, "Equations, Tables and Charts for Compressible Flow," NACA, Report 1135, 1953.
- [2] Hilton, W. F., High-Speed Aerodynamics, New York: Longmans, Green and Company, 1951.
- [3] Foote, J. R., and Ray Holland, Jr., "Preliminary Investigation of the Aerodynamic Effects of Linear Acceleration as Related to the High Speed Track," Chapter 22 of "Studies on Dynamics and Instrumentation of the Holloman Track," AFMDC-TR-59-8, Air Force Missile Development Center, Holloman Air Force Base, New Mexico, April 1959, pp 449-572.
- [4] Eschbach, Ovid W., Handbook of Engineering Fundamentals, 2d ed., New York: John Wiley and Sons, 1952.
- [5] Byrd, Paul F., "Theoretical Wave Drag of Shrouded Airfoils and Bodies," NACA, Technical Note 3718, June 1956.
- [6] Chung, Paul M., and Aemer D. Anderson, "Dissociative Relaxation of Oxygen Over an Adiabatic Flat Plate at Hypersonic Mach Numbers, NASA, Technical Note D-140, April 1960.
- [7] Hansen, C. Frederick, Richard A. Early, Frederick E. Alzofon, and Fred C. Witteborn, "Theoretical and Experimental Investigation of Heat Conduction in Air, Including Effects of Oxygen Dissociation," NASA, Technical Report R-27, 1959.
- [8] Sherman, F. S., "A Low-Density Wind-Tunnel Study of Shock-Wave Structure and Relaxation Phenomena in Gases," NACA, Technical Note 3298, July 1955.
- [9] Schexnayder, Chas. J., Jr., and John S. Evans, "Measurements of the Dissociation Rate of Molecular Oxygen," NASA, Technical Report R-108, 1961.

DISTRIBUTION

AFOSR (SRIL) Wash 25, DC	2	The RAND Corporation 1700 Main Street Santa Monica, Calif	2
Scientific and Technical Information Facility ATTN: NASA Representative (S-AK/DL) P. O. Box 5700 Bethesda, Md	2	ASTIA (TIPCR) Arlington Hall Station Arlington 12, Va	15
Chief, R&D, Dept of the Army ATTN: Scientific Information Branch Wash 25, DC	1	Langley Research Center (NASA) ATTN: Technical Library Langley AFB, Va	1
AFSC (SCRS) Andrews AFB Wash 25, DC	1	Lewis Research Center (NASA) ATTN: Technical Library 21000 Brookpark Road Cleveland 35, Ohio	1
Chairman Canadian Joint Staff (DRB/DSIS) 2450 Massachusetts Avenue NW Wash 25, DC	1	Redstone Scientific Information Center U. S. Army Missile Command Redstone Arsenal, Ala	1
U. S. Naval Research Laboratory ATTN: Library Wash 25, DC	1	Institute of Aeronautical Sciences 2 East 64th Street New York 21, NY	1
Institute of Technology (AU) Library MCLI-LIB, Bldg 125, Area B Wright-Patterson AFB, Ohio	1	Applied Mechanics Reviews Southwest Research Institute 8500 Culebra Road San Antonio 6, Texas	2
ASD (Technical Library) Wright-Patterson AFB, Ohio	1	AFCRL (CRRELA) L. G. Hanscom Field, Mass	1
ARL (Technical Library) Bldg 450 Wright-Patterson AFB, Ohio	2	AEDC (AEOIM) Arnold AF Stn, Tenn	1
High Speed Flight Station (NASA) ATTN: Technical Library Edwards AFB, Calif	1	Signal Corps Engineering Laboratory (SIGFM/EL-RPO) Fort Monmouth, NJ	1
AFFTC (FTOTL) Edwards AFB, Calif	1	Linda Hall Library ATTN: Documents Division 5109 Cherry Street Kansas City 10, Mo	1
Ames Research Center (NASA) ATTN: Technical Library Moffett Field, Calif	1	CIA (OCR Mail Room) 2430 E Street NW Wash 25, DC	2

Detachment 1	1	USAFA (DLIB)	2
Hq, Office of Aerospace Research		U. S. Air Force Academy, Colo	
European Office, USAF			
47 Cantersteen		School of Aeronautical and	1
Brussels, Belgium		Engineering Sciences	
		ATTN: Aero and ES Library	
Hq USAF (AFCIN-3T)	1	Purdue University	
Wash 25, DC		Lafayette, Ind	
Hq USAF (AFRDR-LS)	1	Space Technology Laboratories, Inc.	1
Wash 25, DC		ATTN: Information Services	
		Document Acquisition Group	
Chief, Bureau of Ordnance (Sp-401)	1	P. O. Box 95001	
Dept of the Navy		Los Angeles 45, Calif	
Wash 25, DC			
AFMTC (Tech Library MU-135)	1	Commanding General	1
Patrick AFB, Fla		ATTN: ORDBS-OM-TL 312	
		White Sands Missile Range	
APGC (PGTRIL)	1	NMex	
Eglin AFB, Fla		Ordnance Mission	1
		British Liaison Office	
AFSWC (SWOI)	1	White Sands Missile Range	
Kirtland AFB, NMex		NMex	
AU (AUL-6008)	1	New Mexico State University of	1
Maxwell AFB, Ala		Agriculture, Engineering, and Science	
		ATTN: Library	
RADC (RAALD)	1	University Park, NMex	
ATTN: Documents Library			
Griffiss AFB, NY		University of New Mexico	1
		Government Publications Division	
Naval Research Laboratory	1	University of New Mexico Library	
Dept of the Navy		Albuquerque, NMex	
ATTN: Director, Code 5360			
Wash 25, DC			
Commanding Officer	1	<u>LOCAL</u>	
Diamond Ordnance Fuse Laboratories		NLO	1
ATTN: Technical Reference Section			
(ORDTL 06.33)		RRR	1
Wash 25, DC			
		RRRT	3
Hq OAR (RRON/Col T. M. Love)	1		
Tempo D			
4th & Independence Ave, SW			
Wash 25, DC			

<p>Office of Research Analyses Office of Aerospace Research Holloman AFB, New Mexico</p> <p>GAS DYNAMIC ASPECTS OF AN ENCLOSED HYPERSONIC TEST TRACK May 1963, 83 pp, incl. illus. ORA-63-9 Unclassified Report</p> <p>The gas dynamics related to the movement of a track-guided test vehicle through an evacuated tube are considered preliminarily. Values of pressure, temperature, density, and drag are computed for perfect piston action (over)</p>	<p>UNCLASSIFIED</p> <p>I. Project 5928</p> <p>II. Ray Holland, Jr.</p> <p>Tracks (Aerodynamics) Ranges (Establishments) Hypersonic Flow Shock Waves Supersonic Test Vehicles Aerodynamic Heating</p> <p>UNCLASSIFIED</p>	<p>Office of Research Analyses Office of Aerospace Research Holloman AFB, New Mexico</p> <p>GAS DYNAMIC ASPECTS OF AN ENCLOSED HYPERSONIC TEST TRACK May 1963, 83 pp, incl. illus. ORA-63-9 Unclassified Report</p> <p>The gas dynamics related to the movement of a track-guided test vehicle through an evacuated tube are considered preliminarily. Values of pressure, temperature, density, and drag are computed for perfect piston action (over)</p>	<p>UNCLASSIFIED</p> <p>I. Project 5928</p> <p>II. Ray Holland, Jr.</p> <p>Tracks (Aerodynamics) Ranges (Establishments) Hypersonic Flow Shock Waves Supersonic Test Vehicles Aerodynamic Heating</p> <p>UNCLASSIFIED</p>
<p>Office of Research Analyses Office of Aerospace Research Holloman AFB, New Mexico</p> <p>GAS DYNAMIC ASPECTS OF AN ENCLOSED HYPERSONIC TEST TRACK May 1963, 83 pp, incl. illus. ORA-63-9 Unclassified Report</p> <p>The gas dynamics related to the movement of a track-guided test vehicle through an evacuated tube are considered preliminarily. Values of pressure, temperature, density, and drag are computed for perfect piston action (over)</p>	<p>UNCLASSIFIED</p> <p>I. Project 5928</p> <p>II. Ray Holland, Jr.</p> <p>Tracks (Aerodynamics) Ranges (Establishments) Hypersonic Flow Shock Waves Supersonic Test Vehicles Aerodynamic Heating</p> <p>UNCLASSIFIED</p>	<p>Office of Research Analyses Office of Aerospace Research Holloman AFB, New Mexico</p> <p>GAS DYNAMIC ASPECTS OF AN ENCLOSED HYPERSONIC TEST TRACK May 1963, 83 pp, incl. illus. ORA-63-9 Unclassified Report</p> <p>The gas dynamics related to the movement of a track-guided test vehicle through an evacuated tube are considered preliminarily. Values of pressure, temperature, density, and drag are computed for perfect piston action (over)</p>	<p>UNCLASSIFIED</p> <p>I. Project 5928</p> <p>II. Ray Holland, Jr.</p> <p>Tracks (Aerodynamics) Ranges (Establishments) Hypersonic Flow Shock Waves Supersonic Test Vehicles Aerodynamic Heating</p> <p>UNCLASSIFIED</p>

and for partial piston action at speeds up to the hypersonic. The effects of gas imperfections, viscosity, and wave-reflection are explored. The limiting conditions at which a body in a tube ceases to behave like a piston are defined.	UNCLASSIFIED	and for partial piston action at speeds up to the hypersonic. The effects of gas imperfections, viscosity, and wave-reflection are explored. The limiting conditions at which a body in a tube ceases to behave like a piston are defined.	UNCLASSIFIED
	UNCLASSIFIED		UNCLASSIFIED
and for partial piston action at speeds up to the hypersonic. The effects of gas imperfections, viscosity, and wave-reflection are explored. The limiting conditions at which a body in a tube ceases to behave like a piston are defined.	UNCLASSIFIED	and for partial piston action at speeds up to the hypersonic. The effects of gas imperfections, viscosity, and wave-reflection are explored. The limiting conditions at which a body in a tube ceases to behave like a piston are defined.	UNCLASSIFIED
	UNCLASSIFIED		UNCLASSIFIED